Plant Molecular Biology (2019) 101:129–148
https://doi.org/10.1007/s11103-019-00896-w

Common and specific responses to iron and phosphorus deficiencies in roots of apple tree (*Malus* × *domestica*)

Fabio Valentinuzzi[1] · Silvia Venuti[2] · Youry Pii[1] · Fabio Marroni[2] · Stefano Cesco[1] · Felix Hartmann[1] · Tanja Mimmo[1] · Michele Morgante[2] · Roberto Pinton[2] · Nicola Tomasi[2] · Laura Zanin[2]

Received: 16 December 2018 / Accepted: 24 June 2019 / Published online: 2 July 2019

Abstract

Iron and phosphorus are abundant elements in soils but poorly available for plant nutrition. The availability of these two nutrients represents a major constraint for fruit tree cultivation such as apple (*Malus* × *domestica*) leading very often to a decrease of fruit productivity and quality worsening. Aim of this study was to characterize common and specific features of plant response to Fe and P deficiencies by ionomic, transcriptomic and exudation profiling of apple roots. Under P deficiency, the root release of oxalate and flavonoids increased. Genes encoding for transcription factors and transporters involved in the synthesis and release of root exudates were upregulated by P-deficient roots, as well as those directly related to P acquisition. In Fe-deficiency, plants showed an over-accumulation of P, Zn, Cu and Mn and induced the transcription of those genes involved in the mechanisms for the release of Fe-chelating compounds and Fe mobilization inside the plants. The intriguing modulation in roots of some transcription factors, might indicate that, in this condition, Fe homeostasis is regulated by a FIT-independent pathway. In the present work common and specific features of apple response to Fe and P deficiency has been reported. In particular, data indicate similar modulation of a. 230 genes, suggesting the occurrence of a crosstalk between the two nutritional responses involving the transcriptional regulation, shikimate pathway, and the root release of exudates.

Key Message

For the first time, physiological and transcriptomic response of apple plants to Fe and P deficiencies have been thoroughly characterized and compared. Ionomic and transcriptomic analyses on apple roots have been performed and the data have been implemented with the metabolic profiling of root exudates. Our results highlighted that a physiological and transcriptional link occurs between the responses to Fe and P deficiencies in apple tree roots, which may contribute to the efficient strategy to mobilize nutrients from the soil exhibited by this plant species. Data of the present work highlight that the response to both Fe and P starvation shares common features in the modulation of transcription factors, the shikimate pathway and in the release of root exudates. To the best of our knowledge, this evidence suggests for the first time the existence of a cross talk between Fe and P nutritional pathways in tree plants.

Fabio Valentinuzzi and Silvia Venuti have contributed equally to this work.

Electronic supplementary material The online version of this article (https://doi.org/10.1007/s11103-019-00896-w) contains supplementary material, which is available to authorized users.

✉ Nicola Tomasi
nicola.tomasi@uniud.it

[1] Faculty of Science and Technology, Free University of Bolzano, Piazza Università 5, 39100 Bolzano, Italy

[2] Dipartimento di Scienze Agroambientali, Alimentari e Animali, University of Udine, via delle Scienze 206, 33100 Udine, Italy

Keywords Fe acquisition · P acquisition · RNA-seq · Root exudates · Root uptake · Transcriptomic analyses

Abbreviations

ACO	1-Aminocyclopropane-1-carboxylate oxidase
AGL42	AGAMOUS-like 42
ALMT	Aluminum-activated malate transporter
APR	APS reductase
APS	ATP sulfurylase
Aux/IAAs	Auxin-responsive proteins
bHLH	Basic helix-loop-helix
CHS	Chalcone synthase
CHS	Chalcone synthase
CM	Chorismate mutase
DFR	Dihydroflavonol 4-reductase
ERF	Ethylene response factor
FER	Ferritin
FRD	Ferric reductase defective
FRO	Ferric reduction oxidase
HCT	Hydroxycinnamoyl-CoA shikimate/quinate hydroxycinnamoyl transferase
HXXXD-type AT	HXXXD-type acyl-transferase
IRT	Iron transporter
LPR1	Low phosphate root1
MATE	Multidrug and toxin efflux transporter
MRP	Multidrug resistance-associated protein
MYBs	Myeloblastosis family of transcription factors
NAS	Nicotianamine synthase
NRAMP	Natural macrophage resistant protein
OPT	Oligopeptide transporter
PAP	Purple acid phosphatases
PDR	Pleiotropic drug resistance
PFK	Phosphofructokinase
PFK	Phosphofructokinase
PHO	PHOSPHATE protein
PHT transporters	High-affinity phosphate transporters
PLA2A	Phospholipase A 2A
PS3	P-starvation induced transporter
TCA cycle	Tricarboxylic acid cycle
VIT	Vacuolar iron transporter
ZFP	Zinc-finger protein

Introduction

Apple plant (*Malus* × *domestica* Borkh.) is the main woody fruit species cropped in temperate regions with the third highest worldwide production of edible fruits (FAOSTAT 2013). This fact is mainly ascribable to the high capacity of this plant species to adapt itself to a wide range of soil and climatic conditions. However, the susceptibility of this crop to pathogen attacks (like fungi, Bastiaanse et al. 2015) as well as to the different availability of nutrients in soils (including also the balancing among nutrients) can affect the productivity and fruit quality in the various environments. In a more general context and focusing on the nutritional disorders, it is widely known that, along with nitrogen (N), phosphorus (P) and iron (Fe) deficiencies are the main responsible for yield limitation of crops in the world (Schachtman 1998; Zhang et al. 2010). With respect to Fe, despite being in high amount in most soils, its solubility in the soil solution (*i.e.* plant-available fraction) is very low. Especially in calcareous soils, the high pH reduces the solubility of Fe and therefore its concentration in the soil solution is not enough to sustain the plant requirement.

Also the available fraction of P in soil solution is generally low requiring, therefore, appropriate fertilizations to ensure adequate availability for the crops. However, the efficiency of P fertilization is affected by P precipitation in the soil with cations, as calcium (Ca), aluminium (Al) or Fe, leading to Ca-, Al-. or Fe-phosphates (Raghothama 1999) with also considerable impacts on environment. Considering that calcareous soils account for one-third of the earth's surface (Hansen et al. 2006), the main constraints for successful cultivation of fruit tree crops like apple are represented by the low availability of these two essential elements (Zhang et al. 2010).

Plants have evolved different strategies to cope with nutrient shortage including the release of low- (organic acids, amino acids, sugars, phenolic acids, flavonoids, phytosiderophores, etc.) and high- (polysaccharides, enzymes, etc.) molecular weight organic compounds, generally named root exudates (Bertin et al. 2003; Bais et al. 2006; Lucena et al. 2018). These exudates are able to increase the availability in soil of barely available P and Fe pools by acidifying the rhizosphere, by promoting reduction–complexation processes, ligand exchange reactions and Fe accumulation in plant tissues (Cesco et al. 2010, 2012; Colombo et al. 2013; Mimmo et al. 2014; Zanin et al. 2015). In addition, plants can also increase the spatial availability of nutrients increasing their root surface by either stimulating the growth of fine roots and root hairs or by enhancing mycorrhizal colonization (Neumann and Römheld 2011). At molecular level, plants transcriptionally modulate those genes involved in the specific response to the nutrient starvation. In particular, Fe-deficient plants upregulate a number of genes in order to both increase the capability to acquire Fe and maintain cellular homeostasis (Waters et al. 2014).

In most non-*graminaceous* species, Fe acquisition is mediated by a reduction-based mechanism (called *Strategy I*), which activation led to increase the activities of

ATP-dependent proton pumps, ferric-chelate reductase (FRO) and Fe^{2+} transporter (IRT) all located on plasma membrane of root cells; on the other hand a distinct strategy is operated by grasses (called *Strategy II*) and it involves the root exudation of Fe-chelating molecules, phytosiderophores, and the following uptake in a Fe(III)-complexed form (Marschner et al. 1986). Nevertheless, it has to be considered that up-to-date some reports provide evidence about the existence of a co-occurrence of *Strategy I* and *II* components in plants, suggesting that (although usually one kind of Strategy is preferred) the distinction between *Strategy I*-plants and *Strategy II*-plants is not so obvious (Kobayashi and Nishizawa 2012; Xiong et al. 2013; Zanin et al. 2017).

Colangelo and Lou (2004) showed that Fe-deficient Arabidopsis plants upregulate the transcription factor FIT, which is necessary to regulate the ferric-chelate reductase FRO2 and the Fe^{2+} transporters IRT1 and NRAMP1. Furthermore, in Fe-deficient *Malus xiaojinensis*, Wang et al. (2014a) observed an upregulation of the Fe-uptake related genes only in the earlier period of Fe-deficiency, while genes associated to Fe remobilization process were upregulated in the later period of nutrient shortage. Moreover, they also detected a different expression profile of genes related with hormones, as described also in citrus rootstocks for genes associated not exclusively to hormone metabolism but also to signalling (Licciardello et al. 2013).

The molecular response to P deficiency has been recently investigated in the model plant white lupin (Secco et al. 2014; Wang et al. 2014b; Venuti et al. 2019; Zanin et al. 2019). In these works, besides the upregulation of phosphate transporters, they observed an upregulation of the phenylpropanoid pathway, aluminium-activated malate transporter (ALMT) and multidrug and toxic compound extrusion (MATE) transporter genes correlated with the exudation of citrate and flavonoids and the expression of hormone-related genes. Regarding woody plants, the transcriptomic response of the coniferous tree *Pinus massoniana,* gives a first insight into the molecular mechanisms involved in the response to P-starvation in trees (Fan et al. 2014). Specifically, an alteration in genes related to the lipid metabolism, membrane composition and transcription factors was observed. In addition, they identified a number of upregulated genes either related to P uptake (phosphate transporters) or associated to the transport of sugars, amino acids and organic acids (putatively involved in Pi mobilization and acquisition).

Plant responses to nutrients deficiency have been recently analysed on the basis of large-scale changes in the metabolome (Rellán-Álvarez et al. 2010), proteome (Li et al. 2008; Brumbarova et al. 2008; Donnini et al. 2010; Rodríguez-Celma et al. 2011) and transcriptome (Thimm et al. 2001; O'Rourke et al. 2009). To date, a high-quality draft genome sequence of the domesticated apple has been released (Velasco et al. 2010; Daccord et al. 2017) and therefore a genome wide analyses of transcriptional changes occurring in apple under Fe and P starvation is feasible. Up-to-day many transcriptomic analyses have been conducted in relation to plant response to either Fe (Zamboni et al. 2012; Santos et al. 2013; Li et al. 2014; Zanin et al. 2017) or P (Zheng et al. 2009; O'Rourke et al. 2013; Secco et al. 2014; Zeng et al. 2015) deficiencies. However, the majority of these works were carried out in model and herbaceous plant species, while for our knowledge no transcriptomic analyses have been previously performed on apple under either Fe or P deficiency.

Therefore, in order to identify agronomic strategies for coping with Fe and P deficiency it is crucial to understand the mechanisms underlying the acquisition of these nutrients with particular emphasis to those exploited by plants to overcome these two nutritional disorders. In this study, M9 apple (*Malus* × *domestica* Borkh.) rootstocks were hydroponically grown either in P or in Fe deficiency. Since root exudation is one of the most common strategies adopted by plants to cope with Fe or P deficiency, we firstly aimed at characterizing the exudation pattern of these plants at the first appearance of nutrient-deficiency symptoms. Moreover, to identify the key genes involved in the strategy adopted by apple trees to cope with the two nutrient deficiencies, an RNA-seq approach was undertaken, highlighting the genes differentially expressed in the roots of plants grown under the two nutritional deficiencies.

Materials and methods

Plant growth

Apple rootstocks *(Malus* × *domestica, Borkh.,* M9) were pre-grown in sand, then transferred and grown in hydroponic conditions in a continuously aerated nutrient solution with the following composition: KH_2PO_4 0.25 mM, $Ca(NO_3)_2$ 5 mM, $MgSO_4$, 1.25 mM, K_2SO_4 1.75 mM, KCl 0.25 mM, Fe(III)NaEDTA 20 µM, H_3BO_4 25 µM, $MnSO_4$ 1.25 µM, $ZnSO_4$ 1.5 µM, $CuSO_4$ 0.5 µM, $(NH_4)_6Mo_7O_{24}$ 0.025 µM. Apple trees were grown for 7 days in a full nutrient solution and then for 35 days in Fe-free nutrient solution (−Fe, nutrient solution without Fe(III)NaEDTA), or in a P-free nutrient solution (−P, nutrient solution without KH_2PO_4), or maintained under complete nutrient solution (+P+Fe, as control). The nutrient solution in the pots was renewed twice a week. Plants were grown in a growth chamber under controlled conditions (day: 14 h, 24 °C, 70% relative humidity; night: 10 h, 19 °C, 70% relative humidity).

Characterization of plant growth

Plants were harvested 35 days after the transfer to nutrient-deficient solutions, separating roots and shoots. Fresh weight (FW) of roots and shoots together with the root to shoot ratio were assessed. Light transmittance of fully expanded leaves was determined using a portable chlorophyll meter SPAD-502 (Minolta, Osaka, Japan) and presented as SPAD index values (Supplemental Table S1). Measurements were carried out weekly on young leaves and five SPAD measurements were taken per leaf and averaged.

Collection of root exudates

Apple root exudates were collected 35 days after the transfer to nutrient deficient solutions, at the first appearance of nutrient deficiency symptoms at the leaf level (leaf chlorosis in Fe-deficient plants and bluish leaf veins in P-deficient ones). Plants were therefore removed from the nutrient solutions and roots where washed several times with distilled water in order to remove any traces of nutrient solution. Plants were then transferred in smaller pots containing 250 mL of distilled water (Valentinuzzi et al. 2015a). Root exudates were collected for 24 h continuously aerating the solution and covering the pots with aluminium foil to maintain the roots in the dark to avoid photochemical reactions (Zancan et al. 2006). After 24 h, plants were removed and transferred to pots with fresh nutrient solution. Root exudate solutions were filtered at 0.45 µm (Spartan RC, Whatman), frozen at − 20 °C, lyophilized and resuspended in 2-mL ultrapure distilled water.

Root exudate analyses

Organic acids were separated by high performance liquid chromatography (HPLC) using a cation exchange column (Rezex ROA, Phenomenex), with an isocratic elution with 10-mM H_2SO_4 as carrier solution at a flow rate of 0.6 mL min^{-1}. Organic acids were detected at 210 nm using a Photodiode array detector (PDA 2998, Waters).

Total phenol concentration in root exudates was determined colorimetrically using the Folin-Ciocalteu assay as described by Lowry et al. (1951). Total flavonoid concentration was determined colorimetrically as described by Atanassova et al. (2011).

Total organic carbon (TOC) and total nitrogen (TN) was determined using a Flash EA 1112 elemental analyser (Thermo Scientific).

Elemental analysis

Oven-dried samples (60 °C) of shoots and roots were acid digested with concentrated ultrapure HNO_3 (650 mL L^{-1}; Carlo Erba, Milano, Italy) using a single reaction chamber (SRC) microwave digestion system (UltraWAVE, Milestone, Shelton, CT, USA). Element concentrations were then determined by Inductively Coupled Plasma—Optical Emission Spectrometry (ICP-OES Spectro CirosCCD, Spectro, Germany). Elements quantifications were carried out using certified multi-element standards (CPI International, https://cpiinternational.com). The limits of detection for each element are reported as follows: Al 6.7 mg L^{-1}, B 1.8 mg L^{-1}, Ba 0.1 mg L^{-1}, Ca 2.0 mg L^{-1}, Cu 3.0 mg L^{-1}, Fe 0.4 mg L^{-1}, K 2.0 mg L^{-1}, Li 0.1 mg L^{-1}, Mg 3.0 mg L^{-1}, Mn 0.2 mg L^{-1}, Mo 6.0 mg L^{-1}, Na 1.0 mg L^{-1}, P 4.0 mg L^{-1}, S 4.0 mg L^{-1}, Si 12.0 mg L^{-1}, Sr 0.1 mg L^{-1}, Ti 1.3 mg L^{-1}, Zn 0.2 mg L^{-1}. Tomato leaves (SRM 1573a) and spinach leaves (SRM 1547) have been used as external certified reference material.

RNA extraction, cDNA library preparation and sequencing

Total RNA was extracted from three biological replicates of nine root samples (Control, −P and −Fe plants) using the Spectrum™ Plant Total RNA Kit (Sigma Aldrich). RNA samples were quantified using Qubit™ 2.0 Fluorometer (Life Technology), and RNA integrity was checked with the RNA6000 Nano Assay using the Agilent 2100 Bioanalyzer (Agilent Technologies; RNA requirements for library preparation were $A_{260/280}$ ratio of RNA > 1.8 and RNA Integrity Number, RIN, > 8). cDNA library preparation and sequencing reactions were performed by IGA Technology Services s.r.l. (Udine, Italy). An amount of 2 µg of total RNA was used for library preparation following the Illumina protocol TrueSeq 2.0. Briefly, RNA was fragmented into fragment with an average of 500 bp. mRNA was purified using poly-T beads. The first- and second-strand cDNAs were synthesized and end repaired. Adaptors were ligated after adenylation at the 3′ ends and cDNA templates were enriched by PCR. The 50-bp single-end reads were obtained using an Illumina Hiseq 2000 platform.

Sequence processing

Adapters were removed using cutadapt (http://code.google.com/p/cutadapt/, Martin 2011) and the reads were trimmed for quality with ERNE-FILTER (http://erne.sourceforge.net). Alignment against the genome of *Malus* × *domestica* (http://genomics.research.iasma.it/) using the transcriptome of *Malus* × *domestica* (reference GDDH13 v1.1, including 42140 annotated genes; Daccord et al. 2017) as a guide for transcript assembly was performed with TopHat version 2.0.5 (Kim et al. 2013) with default parameters. Transcript expression was estimated using cufflinks (Trapnell et al. 2010), and differential expression evaluated using cuffdiff

software (q-value < 0.05, n = 3, Trapnell et al. 2012; an overview of the numbers of differentially expressed transcripts is reported in Supplemental Table S2). All RNA-seq expression data are available at the public functional genomics data repository Gene Expression Omnibus (https://www.ncbi.nlm.nih.gov/geo) under the series entry (GSE122554). Genes were annotated according to the annotation of *M. x domestica* GDDH13 v1.1 (available files on the FTP repository: ftp://ftp.bioinfo.wsu.edu/) and were grouped in main functional categories according to the "biological" terms of the Gene Ontology (Ashburner et al. 2000). A cross comparison of singular enrichment analysis (SEACOMPARE) was performed using AgriGO v2.0 software (Tian et al. 2017) on upregulated transcripts, downregulated transcripts and all modulated transcripts in –Fe versus +P+Fe and –P versus +P+Fe (Supplemental Tables S3, S4, S5).

The Arabidopsis homologous to genes commonly modulated by −Fe versus +P+Fe and −P versus +P+Fe (268 genes in total) were analysed on AraNet v2 website (https://www.inetbio.org/aranet/; Lee et al. 2015) using the default parameters to generate a gene network. Moreover to evaluate the occurrence of transcription factor (TF) binding sites within the promoters of the 268 genes, the same list of Arabidopsis homologous genes was loaded on the website of a plant promoter analysis navigator, called PlantPAN 2.0 (http://plantpan2.itps.ncku.edu.tw/; Chow et al. 2015) using the tool "Gene Group Analysis". In the present work the putative interactions between TFs and promoter binding sites are referred to those TFs present in the input gene group.

Real-time reverse transcription–PCR

To validate the RNA-seq data, real-time reverse transcription–PCR (RT-PCR) analyses were performed on apple roots. Therefore, 1 µg of total RNA of each sample was retrotranscribed using 1 pmol of Oligo $d(T)_{23}VN$ (New England Biolabs) and 10.

U M-MulV RNase H for 1 h at 42 °C (Finnzymes) as described in Zanin et al. (2016). Gene-specific primers were designed for the target genes as well as for the housekeeping genes (see Supplemental Table S6). Real-time RT–PCR experiments were carried out in biological triplicates and the reaction was performed by using the SsoFast EvaGreen Supermix (Bio-Rad) as previously described (Valentinuzzi et al. 2015b). Nevertheless, the identity of each amplicon was determined by sequencing. The amplification efficiency was calculated from raw data using LinRegPCR software (Ramakers et al. 2003). The relative expression ratio value was calculated for treated samples relative to the corresponding untreated sample at the same time-point according to the Pfaffl equation (Pfaffl 2001). Standard error values were calculated according to Pfaffl et al. (2002).

Statistical analyses

Results are presented as means of at least three replicates ± standard error (SE). Statistical analysis was performed using Statgraphics (Statpoint technologies, INC., Warrenton, VA, USA). Data were analysed by analysis of variance (ANOVA), and means were compared using SNK's test at $p < 0.01$. Multivariate analyses were carried out by using PAST3.12 software (Hammer et al. 2001). The validity of the PCA models were assessed by the cross-validation approach as previously described (Pii et al. 2015). Transcriptomic data were analysed using cuffdiff (q-value < 0.05 N = 3; Trapnell et al. 2012). All statistically significant transcripts are expressed as positive or negative Log_2FC values (corresponding to up- or down-regulated transcripts, respectively).

Results

Physiological effect of Fe or P deficiency in apple plants

The results of the present study showed that, at the end of the nutritional treatment, Fe and P shortage did not affect significantly the shoot and root biomass and therefore the shoot/root ratio (Supplemental Table S1). As expected, Fe shortage caused a decrease in the leaf chlorophyll content (expressed as units of SPAD index) during the growing period of approximately 20 units compared to the +P+Fe plants (Supplemental Table S1), showing the typical symptoms of Fe chlorosis on young leaves (Fig. 1). On the other hand, P-deficient leaves showed an increased value of SPAD index compared to +P+Fe plants, with characteristic purple-bluish leaf veins (Fig. 1).

Ionomic profile of apple plants

The analyses of both Fe and P concentrations confirmed that the plants were experiencing the imposed nutrient deficiencies (Supplemental Fig. S1). An exploration of the dataset obtained from the elemental analyses was carried out by applying an unsupervised pattern recognition analysis (Principal Component Analysis, PCA) and a model featuring three components, accounting for a total variance of 97.3%, was generated. The scatterplot obtained by combining the Principal Component 1 (PC1—86.36%) and the PC2 (6.81%) displayed a clear separation of the samples in two independent clusters along the horizontal axis (Fig. 2a). In particular, −Fe roots samples were separated from –P and +P+Fe (Fig. 2a), zinc (Zn), copper (Cu) and manganese (Mn) were the main drivers of this clusterization, being significantly more concentrated in –Fe roots (Table 1). On the

Fig. 1 Leaves of apple rootstocks at 35 days after transfer (DAT) to either Fe- or P-deficient nutrient solutions compared to a +P+Fe. **a** Leaves of a P-deficient plant at 35 DAT, **b** Leaves of a +P+Fe plant at 35 DAT, **c** Leaves of a Fe-deficient plant at 35 DAT

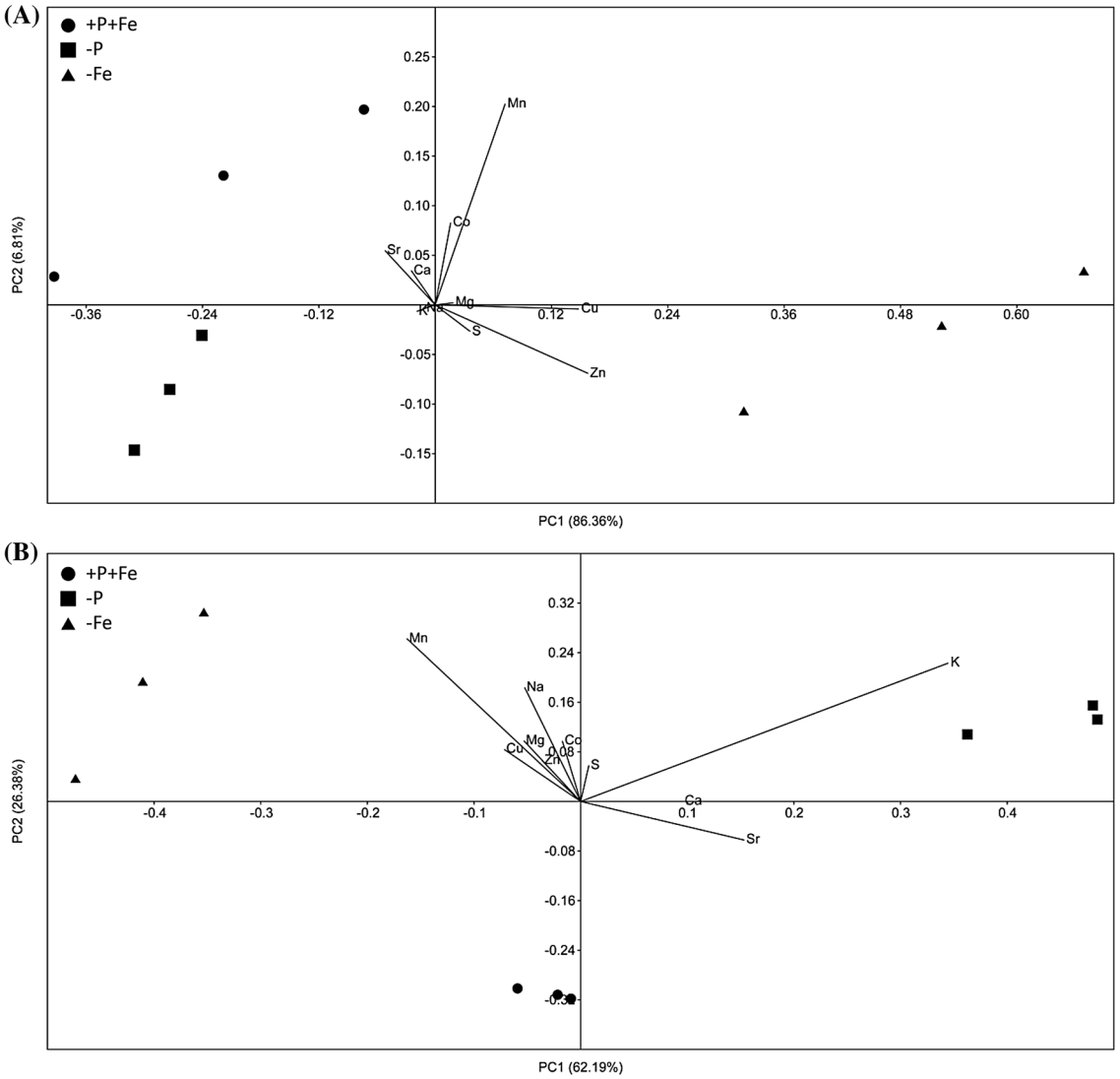

Fig. 2 Principal components analysis (PCA) of apple plants ionome. **a** Biplot representing the modification of the root ionome as a function of the nutritional regime (−P, −Fe, +P+Fe). **b** Biplot representing the modification of the shoot ionome as a function of the nutritional regime (−P, −Fe, +P+Fe)

Table 1 Elements concentration in leaves and roots of apple plants harvested 35 days after the nutrient starvation treatments (P deficiency, −P; Fe deficiency, −Fe; sufficient condition, +P+Fe)

	+P+Fe		−Fe		−P		P value
	Mean	SE	Mean	SE	Mean	SE	
Leaves							
Zn (μg g^{-1})	61.27	5.12	78.1	0.57	65.39	7.56	0.1414
Cu (μg g^{-1})	0.03	0 a	0.04	0 b	0.03	0 a	**0.0029**
Mn (μg g^{-1})	92.13	4.28 a	254.75	18.17 b	112.81	6.83 a	**0.0001**
Ca (mg g^{-1})	30.73	1.52 a,b	24.91	1.78 a	37.59	3 b	**0.0185**
Mg (mg g^{-1})	7.12	0.16 a	10.26	0.14 b	7.94	0.57 a	**0.0019**
S (mg g^{-1})	3.16	0.14	3.92	0.48	4.04	0.16	0.1632
K (mg g^{-1})	4.48	0.03 a	4.1	0.42 a	18.48	1.75 b	**<0.0001**
Co (μg g^{-1})	0.56	0.04	0.73	0.07	0.65	0.01	0.099
Na (mg g^{-1})	0.63	0.05	1.09	0.25	0.81	0.15	0.2222
Sr (μg g^{-1})	51.67	2.76 b	31.17	3.3 a	61.59	3.6 b	**0.0015**
Roots							
Zn (μg g^{-1})	405.2	17.68 a	1345.47	105.83 b	392.8	14.78 a	**<0.0001**
Cu (μg g^{-1})	0.2	0.03 a	0.57	0.09 b	0.19	0.01 a	**0.0029**
Mn (μg g^{-1})	662.6	54.34 a	1225.87	103.3 b	573.6	28.64 a	**0.0011**
Ca (mg g^{-1})	16.47	0.91 b	13.56	0.3 a	15.46	0.15 a,b	**0.0271**
Mg (mg g^{-1})	4.13	0.07	4.71	0.42	4.17	0.01	0.2539
S (mg g^{-1})	4.07	0.21	5.36	0.73	4.49	0.2	0.2049
K (mg g^{-1})	14.21	0.09	12.75	1.11	14.2	0.05	0.2609
Co (μg g^{-1})	1.71	0.12	1.81	0.08	1.46	0.14	0.1765
Na (mg g^{-1})	0.89	0.05	0.8	0.06	0.94	0.04	0.2182
Sr (μg g^{-1})	20.62	3.29	14.51	0.58	19.76	0.83	0.1403

Bold indicate the p values under < 0.05

Values are reported as mean ± SE, six independent replicates were analysed. Statistical significance has been assessed by one-way ANOVA with Tukey post-test ($p < 0.05$). Different letters indicate statistically different values

other hand, the PCA carried out on leaf ionome produced a four components model, accounting for 98.11% of the total variance. The combination of PC1 (62.19%) and PC2 (26.38%) generated a scatter plot displaying three independent clusters, according with the different treatments (−Fe, −P and +P+Fe) along the PC1 (Fig. 2b). The main variables responsible for this separation were Cu, Mn and magnesium (Mg) in the negative direction of the axis, whilst calcium (Ca) and potassium (K) in the positive one (Fig. 2b). Indeed, Cu, Mn and Mg were significantly accumulated in the leaves of –Fe apple plants, whereas Ca and K displayed a higher concentration in the leaf tissue of –P plants (Table 1).

Release of root exudates by apple plants under Fe or P deficiency

Analyses on total carbon (C) and N concentration in apple root exudates provided a preliminary indication on the composition of root exudates released under either Fe or P deficiency. Despite no significant differences were detectable for C and N total content, the qualitative analysis of root

Table 2 Root exudates released by apple roots grown in a full nutrient solution (+P+Fe), phosphorus (−P) and iron-deficient (−Fe) solution at 35 days after transferring the plants to the nutrient solution (DAT)

	+P+Fe	−P	−Fe
	(μmol g^{-1} root FW)		
C released	7.12 ± 2.27 ^{ns}	5.27 ± 1.70 ^{ns}	5.91 ± 0.61 ^{ns}
N released	0.61 ± 0.15 ^{ns}	0.61 ± 0.12 ^{ns}	0.60 ± 0.04 ^{ns}
Oxalate	0.17 ± 0.01^{a}	0.35 ± 0.03^{b}	0.27 ± 0.05^{ab}
Total phenols	3.29 ± 0.95 ^{ns}	3.22 ± 0.61 ^{ns}	1.93 ± 0.29 ^{ns}
Total flavonoids	0.71 ± 0.12^{ab}	1.18 ± 0.25^{b}	0.41 ± 0.13^{a}

Total phenols are expressed as gallic acid equivalents and total flavonoids are expressed as catechin equivalent; FW = fresh weight; mean ± SE. Statistical significance has been assessed by one-way ANOVA with Tukey post-test ($p < 0.05$). Different letters indicate statistically different values

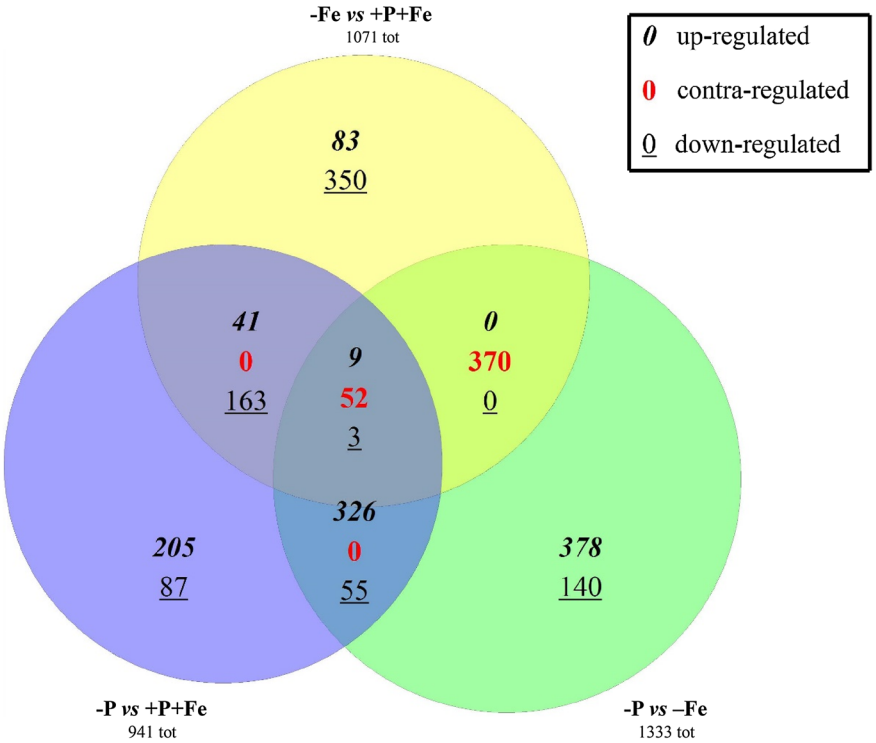

Fig. 3 Venn diagram of three comparisons: −Fe versus +P+Fe, −P versus +P+Fe and −P versus −Fe, the number of differentially expressed transcripts are provided as upregulated (italic font), downregulated (underlined) and contra-regulated (red numbers, N = 3, q-value < 0.05)

exudates highlighted differences among samples for organic acid and flavonoid content. Oxalic acid was the only organic acids present over the detection limit (Table 2) in apple root exudates, with an enhanced release by nutrient deficient plants, especially by –P roots.

Results suggest that phenol efflux is not related to a specific nutrient shortage since they were detectable irrespectively to nutritional status of plants (Table 2). On the other hand, the most abundant release of flavonoids was measured from roots of P-deficient plants, which was significantly higher than the amount released by Fe-deficient plants (Table 2).

Transcriptomic analyses of apple plant roots

For a deep comprehension of the processes that are triggered by either a decreased Fe or P supply, the whole root transcriptome of apple plants in those conditions was analysed by RNA-seq approach. At the end of nutritional treatment (35 DAT), apple roots were sampled and three transcriptomic profiles were obtained and compared each other: −Fe, −P and +P+Fe (this latter used as control condition; $N = 3$).

A total of 194,474,628 reads were obtained and aligned to the *Malus* × *domestica* reference genome (GDDH13 v1.1 whole genome assembly and annotation, available files on the FTP repository:ftp://ftp.bioinfo.wsu.edu/; Daccord et al. 2017). Transcriptomic data were validated selecting randomly 8 differentially expressed transcripts whose expression was checked by real time RT-PCR analyses (Supplemental Table S6).

In comparison to control (+P+Fe), Fe-deficient apple roots showed 1071 differentially expressed genes (−Fe vs. +P+Fe: 209 up-regulated and 862 down-regulated), whilst P starved roots modulated 941 genes (−P vs. +P+Fe: 615 up-regulated and 326 down-regulated, Fig. 3, Supplemental Table S2); Fig. 3 shows that 268 transcripts were modulated in both comparisons (−Fe vs. +P+Fe and −P vs. +P+Fe). The direct comparison of –P transcriptomic profile with –Fe one indicated 1333 differentially modulated transcripts (−P vs. −Fe: 1059 up-regulated and 274 down-regulated). Comparing Fe-deficient response with the P-deficient one, an opposite trend of the gene expression was observed: a. 80% transcripts were downregulated by Fe deficiency, while P deficiency upregulated the majority of its modulated transcripts (a. 65%) (Fig. 3, Supplemental Table S2).

Concerning biological Processes (P categories, according to Gene Ontology, GO), the cross comparison of singular enrichment analysis (SEACOMPARE by AgriGO v2.0 software, Tian et al. 2017) of the whole transcriptional modulation of −Fe versus +P+Fe and −P versus +P+Fe revealed that the "oxidation–reduction process", "single-organism metabolic process", "single-organism process", "metabolic process" and "carbohydrate metabolic process" were the main enriched-P categories to be commonly regulated by both nutritional responses (significant GO P-categories involving more than 10 modulated transcripts

Table 3 Cross comparison of Singular Enrichment Analysis (SEA-COMPARE) of upregulated (above table) and downregulated (below table) transcripts in –Fe versus +P+Fe and/or –P versus +P+Fe (SEA performed using the statistical test method: Fisher, multi test adjustment method: Yekutieli-FDR under dependency, significance level: 0.05)

Up-regulated transcript			CM		-Fe vs +P+Fe		-P vs +P+Fe	
GO Term	Onto	Description	1	2	FDR	Num	FDR	Num
GO:0055114	P	oxidation-reduction process			2.30E-08	34	3.00E-14	88
GO:0044710	P	single-organism metabolic process			5.20E-07	44	7.30E-10	115
GO:0044699	P	single-organism process			0.00056	48	3.10E-05	134
GO:0006979	P	response to oxidative stress			---	---	0.00073	13
GO:0006820	P	anion transport			---	---	0.00074	10
GO:0008152	P	metabolic process			---	---	0.0024	210
GO:0071669	P	plant-type cell wall organization or biogenesis			---	---	0.0043	7
GO:0009664	P	plant-type cell wall organization			---	---	0.0043	7
GO:0006835	P	dicarboxylic acid transport			---	---	0.006	5
GO:0015743	P	malate transport			---	---	0.006	5
GO:0015740	P	C4-dicarboxylate transport			---	---	0.006	5
GO:0015711	P	organic anion transport			---	---	0.018	5
GO:0006811	P	ion transport			---	---	0.018	24
GO:0046942	P	carboxylic acid transport			---	---	0.018	5
Down-regulated transcript			CM		-Fe vs +P+Fe		-P vs +P+Fe	
GO Term	Onto	Description	1	2	FDR	Num	FDR	Num
GO:0055114	P	oxidation-reduction process			1.20E-12	108	0.011	32
GO:0071103	P	DNA conformation change			4.80E-09	21	---	---
GO:0006323	P	DNA packaging			1.30E-08	19	---	---
GO:0006334	P	nucleosome assembly			2.00E-08	18	---	---
GO:0065004	P	protein-DNA complex assembly			2.00E-08	18	---	---
GO:0034728	P	nucleosome organization			2.00E-08	18	---	---
GO:0031497	P	chromatin assembly			2.00E-08	18	---	---
GO:0071824	P	protein-DNA complex subunit organization			2.00E-08	18	---	---
GO:0006333	P	chromatin assembly or disassembly			2.40E-08	18	---	---
GO:0044710	P	single-organism metabolic process			2.10E-07	140	0.022	47
GO:0034622	P	cellular macromolecular complex assembly			2.50E-06	21	---	---
GO:0006461	P	protein complex assembly			2.90E-06	21	---	---
GO:0070271	P	protein complex biogenesis			2.90E-06	21	---	---
GO:0051276	P	chromosome organization			2.90E-06	21	---	---
GO:0006325	P	chromatin organization			4.80E-06	18	---	---
GO:0065003	P	macromolecular complex assembly			8.10E-06	21	---	---
GO:0071822	P	protein complex subunit organization			3.60E-05	21	---	---
GO:0022607	P	cellular component assembly			0.00019	21	---	---
GO:0044699	P	single-organism process			0.001	169	---	---
GO:0043933	P	macromolecular complex subunit organization			0.0013	21	---	---
GO:0008152	P	metabolic process			0.002	288	---	---
GO:0006979	P	response to oxidative stress			0.002	14	---	---
GO:0005975	P	carbohydrate metabolic process			0.003	46	---	---
GO:0009607	P	response to biotic stimulus			0.004	8	---	---
GO:0016043	P	cellular component organization			0.007	33	---	---
GO:0044085	P	cellular component biogenesis			0.0071	21	---	---
GO:1901136	P	carbohydrate derivative catabolic process			0.016	6	---	---
GO:0046348	P	amino sugar catabolic process			0.017	5	---	---
GO:1901072	P	glucosamine-containing compound catabolic process			0.017	5	---	---
GO:1901071	P	glucosamine-containing compound metabolic process			0.017	5	---	---
GO:0006026	P	aminoglycan catabolic process			0.017	5	---	---
GO:0006030	P	chitin metabolic process			0.017	5	---	---
GO:0006032	P	chitin catabolic process			0.017	5	---	---
GO:0006996	P	organelle organization			0.017	21	---	---
GO:0006022	P	aminoglycan metabolic process			0.022	5	---	---
GO:0044264	P	cellular polysaccharide metabolic process			0.025	10	0.0081	7
GO:0006040	P	amino sugar metabolic process			0.026	5	---	---
GO:0071554	P	cell wall organization or biogenesis			0.028	13	---	---
GO:0071840	P	cellular component organization or biogenesis			0.033	33	---	---
GO:0044262	P	cellular carbohydrate metabolic process			0.047	13	0.018	8
GO:0006073	P	cellular glucan metabolic process			---	---	0.0073	7
GO:0044042	P	glucan metabolic process			---	---	0.0073	7
GO:0005976	P	polysaccharide metabolic process			---	---	0.015	7

The domains of biological processes (P) of Gene ontology (GO) are shown, the complete domains of GO (biological processes, functions, cellular components) are shown in Supplemental Tables S3 and S4. A simple colour model (CM) is shown, "1" refers to –Fe versus +P+Fe and "2" to "–P versus +P+Fe"; red colour refers to low values of False Discovery Rate (FDR); yellow colour refers to high FDR values

each, Supplemental Table S5). Other P categories were specifically enriched depending on the nutritional deficiency. In particular among upregulated transcripts, P deficiency enriched those categories related to the transport of organic acids; while under Fe deficiency, P-processes involving chromatin structure, carbohydrate metabolism and other catabolic reactions were mainly over-represented and downregulated (Table 3).

Results indicated that apple roots upregulated several known P-deficiency responsive genes (PSR genes), as those coding for phosphate transporters, transcription factors, phosphatases and others PSR proteins (e.g. PHT1 s; PHO1; SPX-domain containing proteins SPX1, SPX2, SPX3; WRKY75; ABCG37, also known as PDR9; PHO2; LPR1; ALMTs; PAPs; PS2; PS3; SCARECROW; Fig. 5, Table 4, Supplemental Table S7). The P-deficient apple roots showed the upregulation of three transcripts coding for transporters that mediate the release of root exudates: several Multidrug And Toxic compound Extrusion (*MATE*) transcripts (as *FRD3* and other two putative *MATEs*), five transcripts encoding ALuminum-activated Malate Transporters (ALMT) and one transcript encoding pleiotropic drug resistance protein of ABC transporter family (ABCG37, Fig. 5, Table 4, Supplemental Table S7). Under P deficiency, apple plants also showed the upregulation of several transcripts involved in the phenylpropanoid pathway, and more precisely to the scopoletin synthesis (including CHS, DFR, HXXXD-type AT, putative F6′H1, FAH1; Table 4).

Under our conditions, −Fe apple roots modulated a wide range of genes with more than a. 800 genes (75% of –Fe vs. +P+Fe modulated transcripts) specifically responsive to Fe deficiency and only a. 260 genes (24%) in overlapping with those modulated even by P deficiency (Figs. 3, 5, Supplemental Table S2). Concerning the Fe acquisition process, only few known Fe-responsive genes were found modulated in Fe-deficient roots. In particular, transcripts encoding *FIT, VIT, HM3, FER, ALMT, PDR6, TT12, OPT7, YSL3* were found downregulated, while *NAS4, ALMT, bHLH38, ABCG37 (PDR9), OPT3, NRAMP3, BRUTUS (BTS)* were found upregulated by Fe deficiency (Fig. 5, Table 4, Supplemental Table S1). A positive modulation was observed also for *F6′H1, FAH1*, two transcripts involved in the flavonoid synthesis (Table 4).

In total, 268 genes were responsive to both Fe and P deficiency. The hierarchical clustering performed on expression levels of these genes individuated four clusters: *Cluster 1*, upregulated transcripts by both Fe and P deficiencies; *Cluster 2*, upregulated transcripts by Fe deficiency and mainly downregulated by P deficiency; *Cluster 3*, downregulated transcripts by Fe deficiency and upregulated by P deficiency; and *Cluster 4*, downregulated transcripts by both Fe and P deficiencies (Supplemental Table S8). Belonging to *Cluster 1* the most relevant for the acquisition of both nutrients encoded for several transcription factors (bHLHs and MYBs, Aux/IAAs), metabolic enzymes (NAS4, ACO4, HCT, CM, PFK, amylase), transporters (OPT3, MATEs, COPT6 Cu transporter) and ox-red proteins (cytochromes and thioredoxin, Fig. 4). Some interesting genes involved in the Fe acquisition were observed in *Cluster 2*, as those coding for the bHLH038 transcription factor, OPT3, a CYP707A4 cytochrome and extensins. In *Cluster 3* the modulated genes were *VIT, bHLH029, ACO4, PFK3, HCT, CHS, PLA2A and Cytochromes.* The highest number of commonly modulated genes belonged to *Cluster 4* and among these some transcripts encoded for transcription factors (AGL42; MYB; IAA7, -14, -16; ERF13), transporters (PHT1;7, MRP10) and metabolic enzymes (HCT, CM3, APR2, Cytochromes, PLA2A; Supplemental Table S8).

Around half of commonly modulated transcripts (114 of 268 genes) were clustered in functional gene networks by AraNet v2 software (Supplemental Fig. S4). In the network, most of transcription factors clustered together. Central roles for MYB and bHLH transcription factors were highlighted, since they were located as intermediate nodes connecting several TFs to the other nodes (mainly metabolic enzymes). For most of these TFs there are still few functional information available to allow the identification of possible binding sites on promoters of the other commonly modulated gens. Nevertheless, in silico analysis (PlantPAN 2.0; Chow et al. 2015) identified binding sites on promoter of many modulated transcripts which were commonly modulated with TFs: At5g39660 (CDF2), At4g32890 (GATA9), At5g15150 (HAT7), At1g69780 (AtHB13), At5g62165 (AGL42), At2g16720 (MYB7), At1g18330 (RVE7), At5g01380 (Supplemental Table S9).

Discussion

Response of apple roots to P deficiency: P uptake and metabolism

Phosphorus is an essential element for plant nutrition and its lack can strongly limit growth, therefore plants have evolved a plethora of mechanisms, including morphological, physiological and molecular responses, to overcome this situation (Yang and Finnegan 2010; Plaxton and Tran 2011).

As part of the transport, sensing and signalling P network, the upregulation in P-deficient apple roots of several PSR genes (Fig. 5, Table 4, Supplemental Table S7) is in agreement with results obtained in model plants, such as Arabidopsis and lupin (Wu et al. 2003; Wang et al. 2014b; Venuti et al. 2019). In P-deficient apple roots, the upregulations of several phosphate transporters (as PHTs for the Pi-uptake and PHO1 for the Pi loading into the xylem apoplastic space; Hamburger et al. 2002; Nussaume et al. 2011) are key factors

Table 4 Table of most relevant modulated transcripts and reported in "Results" and "Discussion"

Gene ID	FPKM			−Fe vs +P+Fe		−P vs +P+Fe		−P vs −Fe		Symbol	Description
	+P+Fe	−Fe	−P	Log2(FC)	q_value	Log2(FC)	q_value	Log2(FC)	q_value		
MD04G1187600	16.59	26.45	22.45	**0.67**	**0.04**	0.44	0.36	−0.24	0.87	ABCG37 (PDR9)	Pleiotropic drug resistance 9
MD11G1159100	30.73	12.56	84.62	**−1.29**	**0.00**	1.46	0.23	**2.75**	**0.00**	PDR6	Pleiotropic drug resistance 6
MD16G1137900	9.83	15.03	39.63	0.61	0.13	**2.01**	**0.00**	**1.40**	**0.00**	ABCG37 (PDR9)	Pleiotropic drug resistance 9
MD17G1131800	6.35	2.19	11.26	**−1.54**	**0.00**	0.83	0.06	**2.36**	**0.00**	TT12	MATE efflux family protein
MD07G1253900	33.22	22.08	59.82	−0.59	0.15	**0.85**	**0.01**	**1.44**	**0.00**	PS3	Phosphate starvation-induced gene 3
MD06G1133000	6.60	4.02	9.44	−0.72	0.21	0.52	0.43	**1.23**	**0.00**	PHT3;1	Phosphate transporter 3;1
MD14G1149200	2.82	1.22	5.33	**−1.20**	**0.03**	0.92	0.11	**2.12**	**0.00**	PHT3;2	Phosphate transporter 3;2
MD00G1030300	73.47	100.99	146.75	0.46	0.42	**1.00**	**0.02**	0.54	0.38	NRAMP6	NRAMP metal ion transporter 6
MD01G1225900	2.36	0.89	2.90	**−1.41**	**0.01**	0.29	0.89	**1.70**	**0.00**	YSL3	YELLOW STRIPE like 3
MD02G1180400	26.53	57.91	21.53	**1.13**	**0.00**	−0.30	0.71	**−1.43**	**0.00**	NRAMP3	Natural resistance-associated macrophage protein 3
MD06G1080900	18.26	19.90	34.63	0.12	0.99	**0.92**	**0.00**	**0.80**	**0.01**	HMA5	Heavy metal atpase 5
MD13G1244500	20.89	20.80	35.30	−0.01	1.00	**0.76**	**0.01**	**0.76**	**0.02**	HMA2	Heavy metal atpase 2
MD02G1311900	2.47	2.16	20.86	−0.19	0.99	**3.08**	**0.00**	**3.27**	**0.00**	MATE	MATE efflux family protein
MD15G1393900	0.12	0.24	0.89	1.00	1.00	**2.86**	**0.02**	**1.86**	**0.02**	ZF14	MATE efflux family protein
MD05G1360700	21.14	59.02	12.30	**1.48**	**0.00**	**−0.78**	**0.01**	**−2.26**	**0.00**	OPT3	Oligopeptide transporter
MD06G1116800	10.00	4.63	6.87	**−1.11**	**0.00**	−0.54	0.35	0.57	0.33	OPT7	Oligopeptide transporter 7
MD08G1191400	0.70	4.61	0.48	**2.73**	**0.00**	−0.52	0.78	**−3.25**	**0.00**	OPT3	Oligopeptide transporter
MD05G1198100	15.41	9.13	9.20	**−0.76**	**0.03**	**−0.74**	**0.03**	0.01	1.00	PHT1;7	Phosphate transporter 1;7
MD06G1004700	3.63	4.13	6.58	0.19	0.98	**0.86**	**0.05**	0.67	0.19	PHT1;9	Phosphate transporter 1;9
MD07G1046300	0.49	0.64	6.61	0.38	0.98	**3.74**	**0.00**	**3.36**	**0.00**	PHT1;7	Phosphate transporter 1;7
MD13G1213400	136.45	108.56	286.06	−0.33	0.74	**1.07**	**0.01**	**1.40**	**0.00**	ATPT2, PHT1;4	Phosphate transporter 1;4
MD13G1216800	14.75	15.60	27.62	0.08	1.00	**0.91**	**0.00**	**0.82**	**0.01**	PHO1	Phosphate 1
MD13G1216900	25.60	23.87	55.58	−0.10	1.00	1.12	0.06	**1.22**	**0.03**	PHO2	Phosphate 1
MD16G1222100	32.09	29.62	68.01	−0.12	0.99	**1.08**	**0.00**	**1.20**	**0.00**	PHO3	Phosphate 1
MD01G1024600	3.28	15.01	5.78	**2.19**	**0.00**	0.82	0.06	**−1.38**	**0.00**	SULTR2;1	Slufate transporter 2;1
MD08G1177400	3.00	4.93	2.39	0.72	0.11	−0.33	0.84	**−1.05**	**0.01**	SULTR1;3	Sulfate transporter 1;3
MD11G1280200	4.82	3.22	5.70	−0.58	0.31	0.24	0.92	**0.83**	**0.03**	SULTR3;1	Sulfate transporter 3;1
MD15G1355100	28.42	32.97	18.89	0.21	0.90	−0.59	0.09	**−0.80**	**0.00**	SULTR1;3	Sulfate transporter 1;3
MD01G1068100	17.82	29.32	70.27	0.72	0.07	**1.98**	**0.00**	**1.26**	**0.01**	FRO2	Ferric reduction oxidase 2
MD01G1207200	0.40	0.14	1.78	−1.57	1.00	**2.15**	**0.00**	**3.72**	**0.00**	FRO4	Ferric reduction oxidase 4
MD07G1010700	14.02	15.45	37.57	0.14	0.99	**1.42**	**0.00**	**1.28**	**0.00**	FRD3	MATE efflux family protein
MD07G1278100	0.29	0.16	3.39	−0.84	1.00	**3.55**	**0.00**	**4.38**	**0.00**	FRO4	Ferric reduction oxidase 4
MD01G1157700	40.86	26.50	61.49	−0.62	0.10	0.59	0.09	**1.21**	**0.00**	FER4	Ferritin 4
MD04G1164500	2.12	1.66	5.11	−0.35	0.91	**1.27**	**0.01**	**1.62**	**0.00**	FER1	Ferretin 1
MD04G1215600	5.04	9.97	30.16	**0.98**	**0.02**	**2.58**	**0.00**	**1.60**	**0.00**	NAS4	Nicotianamine synthase 4
MD07G1226500	24.15	16.90	29.38	−0.52	0.24	0.28	0.76	**0.80**	**0.01**	FER2	Ferritin 2

Table 4 (continued)

Gene ID	FPKM			−Fe vs +P+Fe		−P vs +P+Fe		−P vs −Fe		Symbol	Description
MD12G1178200	2.07	0.85	5.31	−1.28	0.11	**1.36**	**0.02**	**2.64**	**0.00**	FER1	Ferretin 1
MD12G1178500	4.79	0.81	3.98	**−2.56**	**0.00**	−0.26	0.97	**2.30**	**0.00**	FER1	Ferretin 1
MD13G1268200	6.95	8.60	64.44	0.31	0.99	**3.21**	**0.00**	**2.91**	**0.00**	NAS3	Nicotianamine synthase 3
MD04G1176900	4.15	1.76	3.52	**−1.24**	**0.03**	−0.24	0.97	1.00	0.13	HAD	HAD superfamily, subfamily IIIB acid phosphatase
MD05G1174000	8.35	7.16	16.08	−0.22	0.92	**0.94**	**0.00**	**1.17**	**0.00**	PAP15	Purple acid phosphatase 15
MD06G1142200	7.54	4.66	15.41	−0.69	0.11	**1.03**	**0.00**	**1.72**	**0.00**	PAP27	Purple acid phosphatase 27
MD06G1233400	1.79	0.61	3.49	−1.55	0.09	0.96	0.27	**2.52**	**0.00**	PAP3	Purple acid phosphatase 3
MD09G1195300	20.11	20.54	51.80	0.03	1.00	**1.37**	**0.00**	**1.33**	**0.00**	PS2	Phosphate starvation-induced gene 2
MD12G1023300	28.79	17.50	46.33	−0.72	0.16	0.69	0.19	**1.40**	**0.00**	PAP22	Purple acid phosphatase 22
MD12G1023400	0.18	0.21	2.38	0.17	1.00	**3.70**	**0.00**	**3.54**	**0.01**	PAP20	Purple acid phosphatases superfamily protein
MD12G1192100	0.26	0.73	3.81	1.49	0.26	**3.86**	**0.00**	**2.38**	**0.00**	HAD	HAD superfamily, subfamily IIIB acid phosphatase
MD13G1016100	1.46	1.83	4.21	0.33	0.95	**1.53**	**0.00**	**1.20**	**0.03**	PAP3	Purple acid phosphatase 3
MD13G1231100	1.98	1.38	4.55	−0.52	0.68	**1.20**	**0.01**	**1.72**	**0.00**	PAP23	Purple acid phosphatase 23
MD15G1020000	8.30	6.67	15.47	−0.31	0.80	**0.90**	**0.00**	**1.21**	**0.00**	PAP1	Purple acid phosphatase 12
MD15G1061100	7.69	9.99	29.77	0.38	0.77	**1.95**	**0.00**	**1.58**	**0.00**	–	Pyridoxal phosphate phosphatase-related protein
MD17G1175900	0.82	0.68	5.15	−0.26	1.00	**2.66**	**0.00**	**2.92**	**0.00**	PS2	Phosphate starvation-induced gene 2
MD16G1029700	2.80	3.01	5.60	0.10	1.00	**1.00**	**0.01**	**0.89**	**0.03**	LPR1	Cupredoxin superfamily protein
MD03G1155200	22.31	11.03	22.68	**−1.02**	**0.00**	0.02	1.00	**1.04**	**0.00**	ALMT	Aluminium activated malate transporter family protein
MD03G1155200	22.31	11.03	22.68	**−1.02**	**0.00**	0.02	1.00	**1.04**	**0.00**	ALMT	Aluminium activated malate transporter family protein
MD03G1266500	0.79	0.62	2.29	−0.36	0.97	**1.53**	**0.02**	**1.89**	**0.00**	ALMT	Aluminium activated malate transporter family protein
MD06G1114500	3.30	3.35	35.05	0.02	1.00	**3.41**	**0.00**	**3.39**	**0.00**	ALMT	Aluminium activated malate transporter family protein
MD07G1153600	1.27	3.55	3.16	**1.48**	**0.02**	**1.31**	**0.04**	−0.16	1.00	ALMT	Aluminium activated malate transporter family protein
MD11G1287000	35.97	37.25	86.62	0.05	1.00	**1.27**	**0.00**	**1.22**	**0.00**	ALMT	Aluminium activated malate transporter family protein
MD14G1135700	1.14	2.14	28.46	0.90	0.28	**4.64**	**0.00**	**3.73**	**0.00**	ALMT	Aluminium activated malate transporter family protein
MD14G1191800	20.96	34.13	25.58	**0.70**	**0.04**	0.29	0.81	-0.42	0.51	–	Zinc ion binding
MD10G1294500	13.70	15.68	24.29	0.20	0.93	**0.83**	**0.00**	0.63	0.07	UBC24 (PHO2)	Phosphate 2
MD02G1031100	1.45	0.58	38.84	−1.32	0.13	**4.74**	**0.00**	**6.06**	**0.00**	SPX1	SPX domain gene 1
MD07G1115200	1.11	0.95	8.38	−0.23	1.00	**2.92**	**0.00**	**3.14**	**0.00**	SPX3	SPX domain gene 3
MD15G1124700	69.16	63.56	123.54	−0.12	0.99	**0.84**	**0.00**	**0.96**	**0.00**	SPX2	SPX domain gene 2
MD15G1172700	19.52	12.92	46.99	−0.60	0.21	**1.27**	**0.00**	**1.86**	**0.00**	SPX1	SPX domain gene 1
MD15G1091000	37.96	20.62	40.37	**−0.88**	**0.02**	0.09	1.00	**0.97**	**0.01**	NADP-ME3	NADP-malic enzyme 3
MD09G1019100	44.21	27.45	41.99	**−0.69**	**0.03**	−0.07	1.00	0.61	0.09	SDH2-2	Succinate dehydrogenase 2-2
MD03G1198900	12.64	20.43	12.05	0.69	0.05	−0.07	1.00	**−0.76**	**0.03**	APR1	APS reductase 1
MD09G1110300	8.18	3.70	1.40	**−1.15**	**0.04**	**−2.55**	**0.00**	**−1.41**	**0.02**	APR2	5'adenylylphosphosulfate reductase 2
MD03G1127500	14.51	7.91	29.59	**−0.87**	**0.04**	**1.03**	**0.00**	**1.90**	**0.00**	FIT (BHLH029)	FER-like regulator of iron uptake
MD03G1129100	17.45	15.11	39.53	−0.21	0.94	**1.18**	**0.00**	**1.39**	**0.00**	FIT (BHLH029)	FER-like regulator of iron uptake

Table 4 (continued)

Gene ID	FPKM			−Fe vs +P+Fe		−P vs +P+Fe		−P vs −Fe		Symbol	Description
MD14G1086600	3.18	75.65	8.97	**4.57**	**0.00**	**1.49**	**0.00**	**−3.08**	**0.00**	BHLH038	Basic helix-loop-helix (bHLH) DNA-binding superfamily protein
MD14G1228100	8.42	19.50	6.28	**1.21**	**0.00**	−0.42	0.44	**−1.64**	**0.00**	BTS	Zinc finger protein-related
MD16G1039900	16.91	14.09	34.30	−0.26	0.80	**1.02**	**0.00**	**1.28**	**0.00**	BTS	Zinc finger protein-related
MD03G1088900	6.40	6.89	11.25	0.11	1.00	**0.81**	**0.02**	0.71	0.06	SCL14	SCARECROW-like 14
MD14G1227500	23.74	11.22	18.30	**−1.08**	**0.00**	−0.38	0.73	0.71	0.15	MYB62	myb domain protein 62
MD06G1138500	2.61	2.85	7.43	0.13	1.00	**1.51**	**0.03**	**1.38**	**0.03**	WRKY75	WRKY DNA-binding protein 75
MD00G1188900	2.36	2.65	6.47	0.17	1.00	**1.46**	**0.02**	**1.29**	**0.01**	F6'H1	2-oxoglutarate (2OG) and Fe(II)-dependent oxygenase superfamily protein
MD05G1221300	3.87	15.22	73.57	**1.98**	**0.00**	**4.25**	**0.00**	**2.27**	**0.00**	F6'H1	2-oxoglutarate (2OG) and Fe(II)-dependent oxygenase superfamily protein
MD05G1354000	3.65	4.94	7.18	0.44	0.74	**0.98**	**0.04**	0.54	0.52	ACO4	ethylene-forming enzyme
MD08G1160900	20.61	5.39	16.09	**−1.94**	**0.00**	−0.36	0.71	**1.58**	**0.00**	–	2-oxoglutarate (2OG) and Fe(II)-dependent oxygenase superfamily protein
MD09G1114800	109.76	94.24	152.09	−0.22	0.90	0.47	0.33	**0.69**	**0.04**	ACO4	Ethylene-forming enzyme
MD10G1328100	31.06	36.18	73.59	0.22	0.92	**1.24**	**0.01**	1.02	0.06	ACO4	Ethylene-forming enzyme
MD17G1106300	23.64	3.92	46.32	**−2.59**	**0.00**	**0.97**	**0.03**	**3.56**	**0.00**	ACO4	Ethylene-forming enzyme
MD01G1070400	0.46	0.13	1.48	−1.81	1.00	**1.68**	**0.02**	**3.49**	**0.01**	ACS1	ACC synthase 1
MD06G1090600	2.35	0.65	1.54	**−1.85**	**0.00**	−0.61	0.51	**1.24**	**0.04**	ACS6	1-aminocyclopropane-1-carboxylic acid (acc) synthase 6
MD14G1111500	4.40	1.19	6.54	**−1.88**	**0.00**	0.57	0.43	**2.45**	**0.00**	ACS6	1-aminocyclopropane-1-carboxylic acid (acc) synthase 6
MD07G1214800	2.50	3.85	22.68	0.62	0.50	**3.18**	**0.00**	**2.56**	**0.00**	–	HXXXD-type acyl-transferase family protein
MD13G1014600	0.41	0.09	3.32	−2.21	1.00	**3.01**	**0.00**	5.22	0.39	–	NAD(P)-linked oxidoreductase superfamily protein
MD16G1012000	2.68	1.52	6.88	−0.82	0.43	**1.36**	**0.02**	**2.18**	**0.00**	–	NAD(P)-linked oxidoreductase superfamily protein
MD04G1111500	13.10	5.89	35.05	**−1.15**	**0.00**	**1.42**	**0.00**	**2.57**	**0.00**	CHS	Chalcone and stilbene synthase family protein
MD14G1160800	204.05	118.31	306.59	**−0.79**	**0.03**	0.59	0.74	1.37	0.13	CHS	Chalcone and stilbene synthase family protein
MD14G1160900	5.02	2.41	13.67	−1.06	0.09	**1.45**	**0.00**	**2.50**	**0.00**	CHS	Chalcone and stilbene synthase family protein
MD15G1132100	80.84	42.57	139.78	**−0.93**	**0.00**	0.79	0.15	**1.72**	**0.00**	CHS	Chalcone and stilbene synthase family protein
MD15G1132200	85.47	34.28	216.20	**−1.32**	**0.00**	**1.34**	**0.01**	**2.66**	**0.00**	CHS	Chalcone and stilbene synthase family protein
MD15G1132300	58.81	36.18	87.80	**−0.70**	**0.03**	0.58	0.45	**1.28**	**0.01**	CHS	Chalcone and stilbene synthase family protein
MD05G1292700	0.36	0.32	2.94	−0.15	1.00	**3.02**	**0.00**	**3.18**	**0.00**	–	2-oxoglutarate (2OG) and Fe(II)-dependent oxygenase superfamily protein
MD10G1268500	0.28	0.18	1.68	−0.63	1.00	**2.61**	**0.01**	**3.23**	**0.01**	–	2-oxoglutarate (2OG) and Fe(II)-dependent oxygenase superfamily protein
MD08G1028600	1.65	1.55	5.46	−0.09	1.00	**1.73**	**0.00**	**1.82**	**0.00**	DFR, TT3, M318	Dihydroflavonol 4-reductase
MD05G1292600	2.04	2.46	21.45	0.27	0.97	**3.39**	**0.00**	**3.12**	**0.00**	SRG1	Senescence-related gene 1
MD08G1029500	2.68	6.09	4.27	**1.18**	**0.01**	0.67	0.37	−0.51	0.57	–	NmrA-like negative transcriptional regulator family protein
MD08G1029600	4.45	11.22	8.57	**1.34**	**0.00**	**0.95**	**0.03**	−0.39	0.67	–	NmrA-like negative transcriptional regulator family protein

Table 4 (continued)

Gene ID	FPKM			−Fe vs +P+Fe		−P vs +P+Fe		−P vs −Fe		Symbol	Description
MD02G1136000	22.06	34.74	23.55	**0.65**	**0.04**	0.09	1.00	−0.56	0.10	FAH1	Ferulic acid 5-hydroxylase 1
MD15G1249600	96.14	112.06	67.00	0.22	0.92	−0.52	0.26	**−0.74**	**0.03**	FAH1	Ferulic acid 5-hydroxylase 1
MD04G1232500	3.54	0.84	1.08	**−2.08**	**0.00**	**−1.72**	**0.00**	0.37	0.91	–	Leucine-rich receptor-like protein kinase family protein
MD13G1175800	8.56	7.10	11.75	−0.27	0.84	0.46	0.34	**0.73**	**0.03**	SPL7	Squamosa promoter binding protein-like 7
MD00G1043300	7.62	4.50	5.73	**−0.76**	**0.03**	−0.41	0.50	0.35	0.69	HAM3	GRAS family transcription factor
MD04G1163300	0.45	0.36	1.41	−0.32	1.00	**1.66**	**0.03**	**1.97**	**0.01**	–	GRAS family transcription factor
MD04G1208900	4.49	0.99	51.09	**−2.18**	**0.01**	**3.51**	**0.00**	**5.69**	**0.00**	VIT	Vacuolar iron transporter (VIT) family protein
MD05G1040300	1.19	0.75	3.58	−0.67	0.64	**1.59**	**0.00**	**2.27**	**0.00**	SCL	GRAS family transcription factor (Scarecrow-like protein)
MD10G1024000	116.72	44.77	260.74	**−1.38**	**0.00**	**1.16**	**0.00**	**2.54**	**0.00**	VIT	Vacuolar iron transporter (VIT) family protein
MD11G1098100	8.93	8.13	16.12	−0.14	0.99	**0.85**	**0.00**	**0.99**	**0.00**	SCL	GRAS family transcription factor (Scarecrow-like protein)
MD12G1196300	2.63	1.23	2.29	**−1.10**	**0.01**	−0.20	0.98	0.90	0.09	SCR	SCARECROW
MD12G1223400	0.41	0.04	3.93	−3.52	1.00	**3.25**	**0.02**	6.77	0.72	VIT	Vacuolar iron transporter (VIT) family protein
MD15G1313900	0.50	4.84	18.04	**3.27**	**0.00**	**5.17**	**0.00**	**1.90**	**0.00**	F6'H1	Feruloyl CoA ortho-hydroxylase 1

See Supplemental Table S7 for addition information; bold numbers referred to significant modulations (q-value < 0.05, N = 3)

of plant response to increase the efficiency of Pi root uptake (Hirsch et al. 2006). In addition to PHO1, other SPX-domain containing proteins were positively modulated by P deficiency. The SPX domains are found in a variety of proteins involved in the transduction of P signal (Barabote et al. 2006; Duan et al. 2008; Chiou and Lin 2011) and related to Pi homeostasis (Secco et al. 2012). In particular SPX1, SPX2 and SPX4 proteins interact and modulate the activity of PHR1, the primary MYB-transcription factor mediating response to P deficiency in plants (Lv et al. 2014; Puga et al. 2014; Wang et al. 2014c). Another gene to be upregulated by P deficiency coded for PHO2, which participates to the post-transcriptional control of PHT abundance (Lin et al. 2008, for review see Gu et al. 2016). Concerning enzymes known to be induced as an adaptive response to Pi starvation (Baldwin et al. 1999, 2001), the transcriptomic analyses highlighted the strong upregulation of a *PS3* (*Phosphate Starvation-induced 3* gene encoding glycerol-3-phosphate permease 1) and several acid phosphatases (including *Phosphate Starvation-induced 2*, *PS2* transcripts). During Pi starvation, the synthesis and secretion of extracellular acid phosphatases increase to allow an efficient remobilization of P from P-enriched organic compounds (Duff et al. 1994; Tang et al. 2013). Results showed also the upregulation of others important key players in root P-sensing, as transcripts encoding LPR1 (a multicopper oxidases), WRKY75 (a transcription factor for P acquisition and root development) and SCARECROW (a GRAS transcription factors, key regulator of root patterning and stem-cell maintenance; for review see Rouached et al. 2010). These proteins are known to be involved in the P sensing and signalling pathway upon P limitation although their interaction network still remains poorly understood.

A further part of the mechanism adopted by P deficient plants to overcome the nutrient shortage is the release of root exudates in the rhizosphere that contribute to nutrient bioavailability in the soil solution. Very few information is available on the release of root exudates by woody plants (Sandnes et al. 2005), especially by apple trees (Zhang et al. 2007). In the present study, a greater capability to release oxalate was observed by P-deficient apple roots than by control roots (+P+Fe, Table 2), and oxalate was the sole carboxylate detectable in apple root exudates. The root release of oxalate might contribute to the solubilisation of Ca/Al/Fe–P minerals, Fe-(hydr)oxides, as well as the release of the Pi adsorbed onto soil colloids by ligand exchange reaction (Gerke 2000).

Beside carboxylates, also phenols can increase P availability in the soil by competing with Pi for sorption sites (Nannipieri et al. 2008) and therefore, their release under P-deficiency seems to be a strategy adopted also by apple trees (Table 2). In agreement with this observation (Table 2), the transcriptomic analyses showed the upregulation of

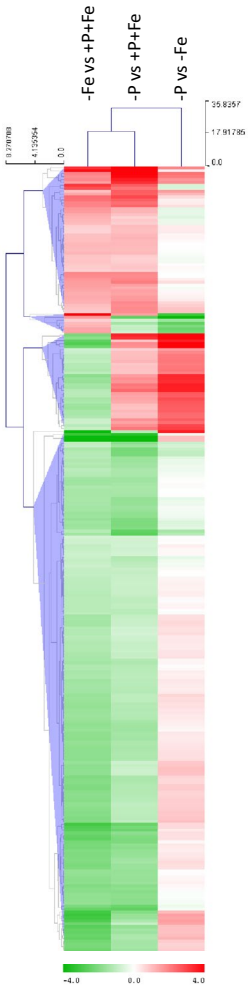

Cluster name	Most relevant transcripts
Cluster 1 ↑Fe ↑P	NAS4 (NICOTIANAMINE SYNTHASE 4) AMY2 (ALPHA-AMYLASE-LIKE 2) MYBs (MYB102; MYB58); ALMT (Al-activated malate transporter) F6'H1 (Feruloyl CoA ortho-hydroxylase) EPR1 (EARLY-PHYTOCHROME-RESPONSIVE1) HSP70 (heat shock protein 70) SEN1 (SENESCENCE 1) MLP31 (MLP-LIKE PROTEIN 31) CDF2 (CYCLING DOF FACTOR 2) polygalacturonase, putative fumarylacetoacetate hydrolase Cytochromes; NSP5 (Nitrile-specifier protein 5) TRX2 (THIOREDOXIN 2) EXLB1 (ARABIDOPSIS THALIANA EXPANSIN-LIKE B1) COPT6 (copper transporter)
Cluster 2 ↑Fe ↓P	bHLH038, transcription factor GLIP1 (GDSL LIPASE1) CYP707A4 cytochrome ATOPT3 (OLIGOPEPTIDE TRANSPORTER) Pollen Ole e 1 allergen and extensins
Cluster 3 ↓Fe ↑P	ACO4 (1-aminocyclopropane-1-carboxylate oxidase) PFK3 (PHOSPHOFRUCTOKINASE 3) bHLH029 (FER-LIKE REGULATOR OF IRON UPTAKE) HCT (HYDROXYCINNAMOYL-COA SHIKIMATE/QUINATE HYDROXYCINNAMOYL TRANSFERASE) PLA2A (PHOSPHOLIPASE A 2A) Cytochromes CHS (4-hydroxycoumarin synthase) GSTU7 (GLUTATHIONE S-TRANSFERASE TAU 7) MMP (MATRIX METALLOPROTEINASE) VIT (Vacuolar iron transporter)
Cluster 4 ↓Fe ↓P	AGL42 (AGAMOUS LIKE 42) Cytochromes APR2 (5ADENYLYLPHOSPHOSULFATE REDUCTASE 2) MYB transcription factors HCT (HYDROXYCINNAMOYL-COA SHIKIMATE/QUINATE HYDROXYCINNAMOYL TRANSFERASE); IAA7, IAA14, IAA16 (INDOLE-3-ACETIC ACID INDUCIBLE transcription factors) ERF13 (ETHYLENE-RESPONSIVE ELEMENT BINDING FACTOR 13); CLAVATA1 receptor kinase (CLV1) PLA2A (PHOSPHOLIPASE A 2A) MRP10 (ATPase, coupled to transmembrane movement of substances) LBD41 (LOB DOMAIN-CONTAINING PROTEIN 41) CM3 (chorismate mutase 3); PHT1;7 (phosphate transporter 1;7)

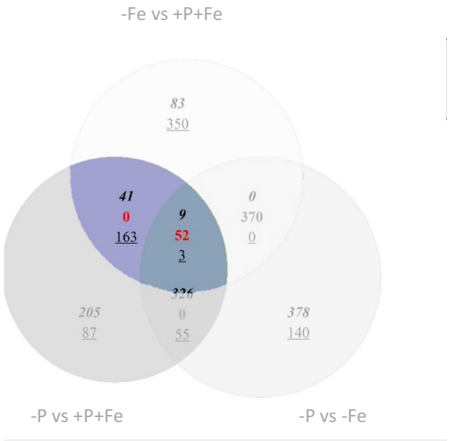

Fig. 4 Hierarchical clustering (HCL) of overlapping genes regulated by both Fe deficiency and by P deficiency in apple roots. The modulation of 268 genes was shared by both nutritional stresses, as indicated in the colour part of Venn diagram (−Fe versus +P+Fe and −P versus +P+Fe intersection as reported in Fig. 3, N = 3, q-value < 0.05) For each hierarchical cluster, the most representative transcripts are indicated (HCL analysis: Euclidean distance, linkage method: average linkage, colour scale refers to the intensity of modulation, as Log_2FC; green colour refers to downregulated transcripts; red colour refers to upregulated transcripts). The full list of clustered transcripts is provided as Supplemental Table S8

several genes involved in the biosynthesis (phenylpropanoid pathway) and efflux of root exudates (Table 4). In Arabidopsis, the F6′H1 and ABCG37 play a crucial role to mediate respectively the synthesis and the root exudation of scopoletin, a coumarin acting as Fe-chelator in the rhizosphere (Schmid et al. 2014; Fourcroy et al. 2014). In plants, along with ABCG37, also MATE and ALMT transporters have been characterized to be the main components for the root efflux of aluminium (Al)/Fe-chelators in the rhizosphere (as organic acids and phenols, Liu et al. 2009; Fourcroy et al. 2014; Durrett et al. 2007). Hence, present data indicate that, at molecular and physiological levels, P-deficient apple trees activate pathways for the synthesis and increase the release of these compounds acting as an efficient strategy to promote the external Pi-solubility from mineral sources (Gottardi et al. 2013; Wang et al. 2014b; Venuti et al. 2019).

Interestingly, Ca and K displayed a higher concentration in the leaf tissue of –P plants (Table 1). Despite the basis of this phenomenon has not yet been clarified, experimental evidence obtained in both rice and grapevine plants grown in field conditions reported the accumulation of both Ca and K at leaves level upon P shortage (Rose et al. 2016; Baldi et al. 2018). In addition, a higher concentration of Ca was also detected in strawberry fruits obtained from plants grown in P deficiency (Valentinuzzi et al. 2015b).

Response of apple roots to Fe deficiency: Fe uptake and metabolism

To cope with Fe-limiting conditions in the rhizosphere, plants have developed several mechanisms that promote and facilitate Fe availability acting on metal acquisition,

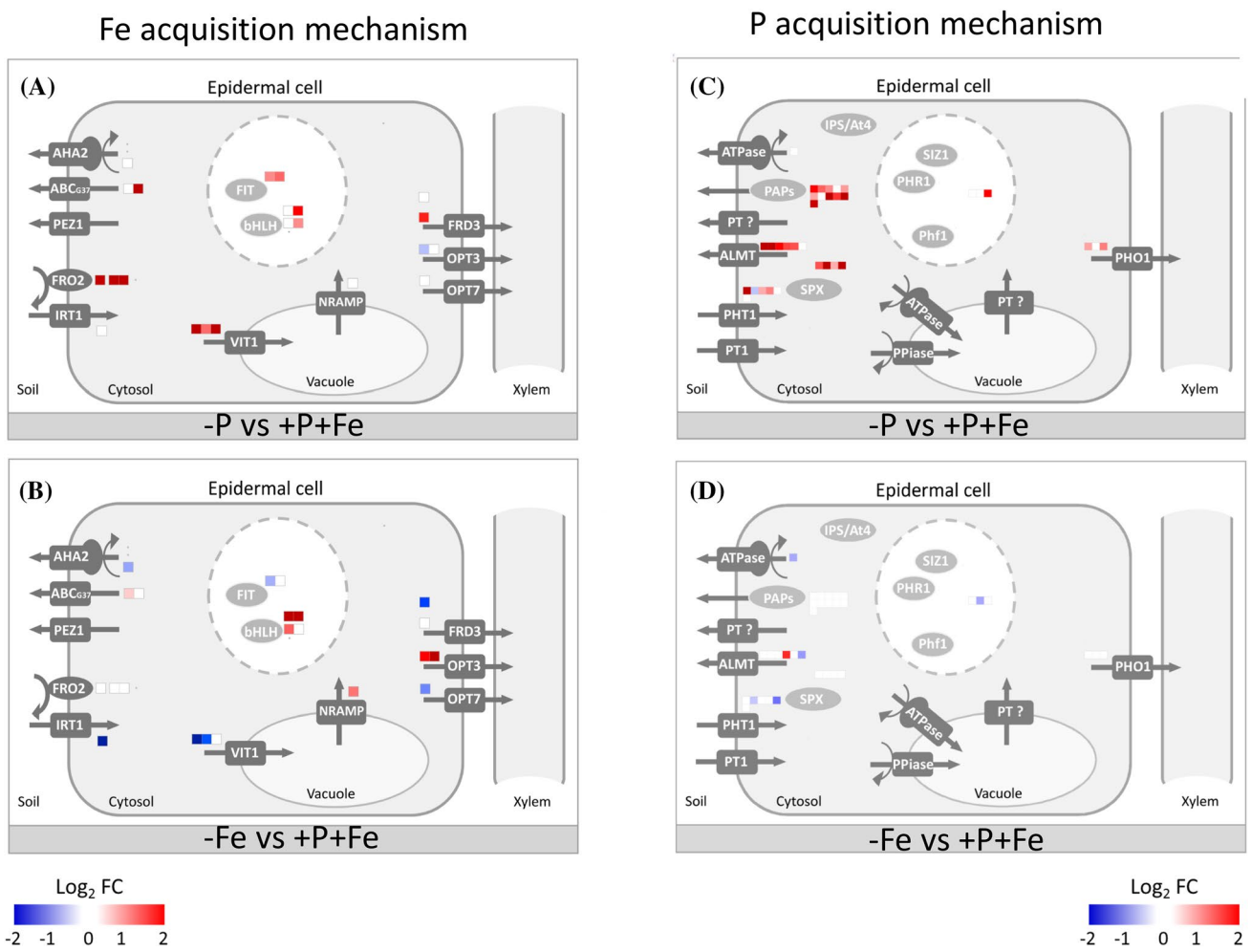

Fig. 5 Mapping of transcriptional modulation on schematic models of Fe-acquisition mechanism (**a**, **b**) and P-acquisition mechanism (**c**, **d**) in root cells. Transcriptional modulation is related to differentially modulated transcripts in −P versus +P+Fe (**a**, **c**) and −Fe versus +P+Fe (**b**, **d**). Colour scale refers to the Log_2 FC values of differentially expressed transcripts: red colour refers to upregulated transcripts, while in blue are shown downregulated transcripts (N = 3, q-value < 0.05)

regulation, storage and allocation of Fe in plants. Previous evidence in apple indicated that this species is highly responsive to Fe deficiency within the first 2 days, while a prolonged condition of Fe shortage can attenuate the response (Wang et al. 2014a). In agreement with this observation, after 5 weeks of Fe deficiency, apple roots did not show changes in the expression of *IRT1* and *FRO2*, the two main genes involved in the *Strategy I* response, but rather an intriguing modulation of regulatory network of Fe homeostasis. It is known that in Arabidopsis, the transcription factor FIT acts with binding partners, i.e. several other bHLHs (forming heterodimers with bHLH038, -039, -100, -101; and interacting with others as bHLH018, -019, -020, -025; Yuan et al. 2008; Wang et al. 2013; Cui et al. 2018). In apple different transcripts encoding bHLHs were found to be regulated by Fe deficiency. Three transcripts homologous to *AtbHLH038* and *AtbHLH093* were upregulated in apple roots, while *bHLH029* (homologous to *AtFIT*) and several other *bHLHs* were concomitantly downregulated by Fe deficiency. As reported for bHLH100 and bHLH101, this data might suggest that also bHLH038 and *AtbHLH093* might have regulatory roles independent from FIT interaction (Sivitz et al. 2012). In plants, the regulation of Fe homeostasis is also under a FIT-independent signalling pathway, a network involving bHLHs and ZFP proteins (as POPEYE and BRUTUS; Long et al. 2010). The positive regulation in apple roots of *bHLH038* and *BRUTUS* after 5 weeks of Fe deficiency might provide new insight into the Fe regulatory mechanism involved in the late response.

Several transporters for the metal transport and mobilization in plants were positively induced, as well some transcripts involved in the phenylpropanoid synthesis (Table 4). This observation indicates that the mechanisms for the release of Fe-chelating compounds and the Fe mobilization

inside the plants were active (Curie and Mari 2017). Nevertheless, under Fe-deficiency the profiling analysis of root exudates indicated that the flavonoid release was even lower than that released by control roots (+P+Fe); while the oxalate amount was slightly increased (Table 2). The exudation of carboxylates as physiological response to Fe starvation has been widely assessed in plants (Jones 1998; Mimmo et al. 2014; Valentinuzzi et al. 2015c; Adeleke et al. 2017). In particular, the oxalate release under Fe deficiency was previously observed also from grapevine root (López-Rayo et al. 2015). On the other hand, the metal storage and sequestration in the vacuole was limited (as suggested by the downregulation of several VITs and Ferritin genes), also the Fe concentration in plant tissues confirmed a severe condition of Fe shortage (Supplemental Fig. S1). As expected, the concentration of other metals (as Zn, Cu, Mn) increased under Fe shortage and this behaviour was also observed in other plant species (Tomasi et al. 2014; Pii et al. 2015). In apple, this pattern might be consequence of the upregulation of genes coding for metal transporters (COPT6, NRAMP3; Supplemental Table S7) and to the necessity of root cells to compensate the cationic uptake for the unbalanced micronutrients availability (Csog et al. 2011; Tomasi et al. 2014) in addition, such micronutrients accumulation might be also ascribable to the low specificity of IRT1 that, beside Fe(II), can also transport Mn, Zn, Cu and Cd (Korshunova et al. 1999). The overaccumulation of Cu and Mn occurred also at the leaf level, suggesting that the upregulation of several genes involved in the synthesis and transport of chelating agents (e.g. nicotianamine) were active to distribute these metals within plant (e.g. Cu–nicotianamine complex, Curie et al. 2009).

Similarities and differences of plant response to Fe deficiency and P deficiency

To understand cross interactions between Fe and P deficient responses in apple roots, particular attention has been paid to those genes commonly modulated by both nutritional conditions, −Fe versus +P+Fe and −P versus +P+Fe. In total, 268 genes were responsive to both Fe and P deficiencies. The hierarchical clustering of this modulation individuated four clusters. In particular the common upregulation by both nutritional deficiencies of *MYB, NAS, F6'H1, ALMT, COPT*, is an interesting indication of a cross-talk among the two nutritional pathways and might suggest a novel role of transcription factors (as MYBs) in the modulation of both Fe and P acquisition mechanisms (Briat et al. 2015; Supplemental Fig. S4). Moreover the common upregulation of *ALMT*, as main candidate transporter for the carboxylate efflux (Sharma et al. 2016), is consistent with the increase of oxalate release (Table 2). The two nutritional deficiencies also shared the common downregulation of some transcripts, as *CLV1, AGL42, IAAs, ERF13, LBD41, CM3* and *HCT*. The modulation of these transcripts indicate that, in apple roots, the Fe and P nutritional pathway shared a further link in the regulation processes being either responsive to hormonal status, as auxin and ethylene, and subject to an alteration of root system architecture.

Of great relevance for the phenolic and flavonoid synthesis is the common modulation of several enzymes related to the shikimate pathway, as CM3, HCT, F6′H1, and especially the common upregulation of F6′H1 is considered to play an essential role for the synthesis of coumarins (Schmid et al. 2014). However, P-deficient roots strongly upregulated also an isoform of *ABCG37* that mediates coumarin release and this observation might indicate that this transporter is involved in the high release of flavonoids by P-deficient roots more than Fe deficient ones.

Opposite modulation was observed between the two nutritional responses for the transcription factor (*bHLH029)* and for the transporters *(VIT, OPT3*). Their role in the Fe acquisition is well known (Sivitz et al. 2012; Jakoby et al. 2004; Mendoza-Cózatl et al. 2014; Zhai et al. 2014; Kim et al. 2006) while scarce information is available about their involvement in the P acquisition (Supplemental Fig. S4, Supplemental Table S9). Under P deficiency, plants did not increased the Fe content, while Fe deficient apple plants showed an overaccumulation of P both in roots and in shoots. An antagonistic behaviour between Fe and P content was previously reported in other Fe-deficient plants (Zheng et al. 2009; Zanin et al. 2017). It is plausible that this behaviour (Fe and P content balance) might evolve during the time of treatment and, depending on the exudation pattern, it might be delayed in P deficient plants in comparison to Fe deficient ones. Nevertheless, we cannot exclude that after a long period of Fe-deficiency, plants have worn down their response, suggesting that the two nutrient deficiencies modulate at different times their physiological and molecular responses.

In conclusion, the data obtained within the present work highlight that the response to both Fe and P starvation shares common features in the modulation of transcription factors, the shikimate pathway and in the release of root exudates. To the best of our knowledge, this evidence suggests for the first time the existence of a crosstalk between Fe and P nutritional pathways in tree plants.

Acknowledgements Research was supported by grants from Italian MIUR (FIRB-Programma "Futuro in Ricerca" RBFR127WJ9), Free University of Bolzano (TN5056). RNA sequencing analyses were performed at the Institute of Applied Genomics (IGA, Udine).

Author contributions FV, SV, YP, FH, LZ conducted experiments; FV, SV, SC, TM, RP, NT and LZ conceived and designed research; FV, SV,

YP, FM, MM and LZ analysed -omic data. FV, YP, LZ, NT wrote the manuscript. All authors read and approved the manuscript.

Data availability All RNA-seq expression data are available at the public functional genomics data repository Gene Expression Omnibus (https://www.ncbi.nlm.nih.gov/geo) under the series entry (GSE122554; link:https://www.ncbi.nlm.nih.gov/geo/query/acc.cgi?&acc=GSE122554).

Compliance with ethical standards

Conflict of interest The authors have no conflict of interest to declare.

References

Adeleke R, Nwangburuka C, Oboirien B (2017) Origins, roles and fate of organic acids in soils: a review. South Afr J Bot 108:393–406

Ashburner M, Ball CA, Blake JA et al (2000) Gene ontology: tool for the unification of biology. Nat Genet 25:25–29

Atanassova M, Georgieva S, Ivancheva K (2011) Total phenolic and total flavonoid contents, antioxidant capacity and biological contaminants in medicinal herbs. J Univ Chem Technol Metall 46:81–88

Bais HP, Weir TL, Perry LG, Gilroy S, Vivanco JM (2006) The role of root exudates in rhizosphere interactions with plants and other organisms. Annu Rev Plant Biol 57:233–266

Baldi E, Miotto A, Ceretta CA et al (2018) Soil-applied phosphorous is an effective tool to mitigate the toxicity of copper excess on grapevine grown in rhizobox. Sci Hortic 227:102–111

Baldwin JC, Karthikeyan AS, Raghothama KG (1999) LePS3, a novel phosphate starvation induced gene in tomato (abstract no. 937). Annual American Society of Plant Physiologists Meeting, July 24–28, Baltimore. American Society of Plant Physiologists, Rockville, MD, p 190

Baldwin JC, Karthikeyan AS, Raghothama KG (2001) LePS2, a phosphorus starvation-induced novel acid phosphatase from tomato. Plant Physiol 125:728–737

Barabote RD, Tamang DG, Abeywardena SN et al (2006) Extra domains in secondary transport carriers and channel proteins. Biochim Biophys Acta (BBA) Biomembr 1758:1557–1579

Bastiaanse H, Muhovski Y, Mingeot D, Lateur M (2015) Candidate defense genes as predictors of partial resistance in 'Président Roulin' against apple scab caused by *Venturia inaequalis*. Tree Genet Genomes 11:125

Bertin C, Yang X, Weston L (2003) The role of root exudates and allelochemicals in the rhizosphere. Plant Soil 256:67–83

Briat JF, Rouached H, Tissot N, Gaymardand F, Dubos C (2015) Integration of P, S, Fe, and Zn nutrition signals in *Arabidopsis thaliana*: potential involvement of PHOSPHATE STARVATION RESPONSE1 (PHR1). Front Plant Sci 6:290

Brumbarova T, Matros A, Mock H-P, Bauer P (2008) A proteomic study showing differential regulation of stress, redox regulation and peroxidase proteins by iron supply and the transcription factor FER. Plant J 54:321–334

Cesco S, Neumann G, Tomasi N, Pinton R, Weisskopf L (2010) Release of plant-borne flavonoids into the rhizosphere and their role in plant nutrition. Plant Soil 329:1–25

Cesco S, Mimmo T, Tonon G et al (2012) Plant-borne flavonoids released into the rhizosphere: impact on soil bio-activities related to plant nutrition. A review. Biol Fertil Soils 48:123–149

Chiou T-J, Lin S-I (2011) Signaling network in sensing phosphate availability in plants. Annu Rev Plant Biol 62:185–206

Chow CN, Zheng HQ, Wu NY, Chien CH, Huang HD, Lee TY et al (2015) PlantPAN 2.0: an update of plant promoter analysis navigator for reconstructing transcriptional regulatory networks in plants. Nucleic Acids Res 44:1154

Colangelo EP, Lou Guerinot M (2004) The essential basic helix-loop-helix protein FIT1 is required for the iron deficiency response. Plant Cell 16:3400–3412

Colombo C, Palumbo G, He J-Z, Pinton R, Cesco S (2013) Review on iron availability in soil: interaction of Fe minerals, plants, and microbes. J Soils Sediments 14:1–11

Csog Á, Mihucz VG, Tatár E et al (2011) Accumulation and distribution of iron, cadmium, lead and nickel in cucumber plants grown in hydroponics containing two different chelated iron supplies. J Plant Physiol 168:1038–1044

Cui Y, Chen CL, Cui M, Zhou WJ, Wu HL, Ling HQ (2018) Four IVa bHLH transcription factors are novel interactors of FIT and mediate JA inhibition of iron uptake in *Arabidopsis*. Mol Plant 11:1166–1183

Curie C, Mari S (2017) New routes for plant iron mining. New Phytol 214:521–525

Curie C, Cassin G, Couch D et al (2009) Metal movement within the plant: contribution of nicotianamine and yellow stripe 1-like transporters. Ann Bot 103:1–11

Daccord N, Celton JM, Linsmith G et al (2017) High-quality de novo assembly of the apple genome and methylome dynamics of early fruit development. Nat Genet 49:1099–1106

Donnini S, Prinsi B, Negri AS, Vigani G, Espen L, Zocchi G (2010) Proteomic characterization of iron deficiency responses in *Cucumis sativus* L. roots. BMC Plant Biol 10(1):268

Duan K, Yi K, Dang L, Huang H, Wu W, Wu P (2008) Characterization of a sub-family of *Arabidopsis* genes with the SPX domain reveals their diverse functions in plant tolerance to phosphorus starvation. Plant J 54:965–975

Duff SMG, Sarath G, Plaxton WC (1994) The role of acid phosphatase in plant phosphorus metabolism. Physiol Plant 90:791–800

Durrett TP, Gassmann W, Rogers EE (2007) The FRD3-mediated efflux of citrate into the root vasculature is necessary for efficient iron translocation. Plant Physiol 144:197–205

Fan F, Cui B, Zhang T, Qiao G, Ding G, Wen X (2014) The temporal transcriptomic response of *Pinus massoniana* seedlings to phosphorus deficiency. PLoS ONE 9:e105068

FAOSTAT (2013) Statistical database of the food and agricultural organization. Available online at http://faostat.fao.org/site/567/DesktopDefault.aspx%3FPageID=567%23ancor

Fourcroy P, Sisó-Terraza P, Sudre D et al (2014) Involvement of the ABCG37 transporter in secretion of scopoletin and derivatives by *Arabidopsis* roots in response to iron deficiency. New Phytol 201:155–167

Gerke J (2000) Mathematical modelling of iron uptake by Graminaceous species as affected by iron forms in soil and phytosiderophore efflux. J Plant Nutr 23:1579–1587

Gottardi S, Tomasi N, Pinton R et al. (2013) Characterisation of a genistein transporter in roots of Lupin plants. Proceedings book of the 17th international plant nutrition colloquium and boron satellite meeting, Sabanci University, Istanbul, Turkey, 19–22 Aug 2013, p 27–28

Gu M, Chen A, Sun S, Xu G (2016) Complex regulation of plant phosphate transporters and the gap between molecular mechanisms and practical application: what is missing? Mol Plant 9:396–416

Hamburger D, Rezzonico E, MacDonald-Comber Petetot J, Somerville C, Poirier Y (2002) Identification and characterization of the *Arabidopsis PHO1* gene involved in phosphate loading to the xylem. Plant Cell 14:889–902

Hammer Ø, Harper DAT, Ryan PD (2001) PAST: paleontological statistics software package for education and data analysis. Palaeontol Electron 4(1):9

Hansen N, Hopkins BG, Ellsworth JW, Jolley VD (2006) Iron nutrition in field crops. In: Barton LL, Abadia J (eds) Iron nutrition in plants and rhizospheric microorganisms. Springer, Dordrecht, pp 61–83

Hirsch J, Marin E, Floriani M et al (2006) Phosphate deficiency promotes modification of iron distribution in *Arabidopsis* plants. Biochimie 88:1767–1771

Jakoby M, Wang HY, Reidt W, Weisshaar B, Bauer P (2004) FRU (BHLH029) is required for induction of iron mobilization genes in *Arabidopsis thaliana*. FEBS Lett 577:528–534

Jones DL (1998) Organic acids in the rhizosphere—a critical review. Plant Soil 205:25–44

Kim SA, Punshon T, Lanzirotti A et al (2006) Localization of iron in Arabidopsis seed requires the vacuolar membrane transporter VIT1. Science 314:1295–1298

Kim D, Pertea G, Trapnell C, Pimentel H, Kelley R, Salzberg SL (2013) TopHat2: accurate alignment of transcriptomes in the presence of insertions, deletions and gene fusions. Genome Biol 14:R36

Kobayashi T, Nishizawa NK (2012) Iron uptake, translocation, and regulation in higher plants. Annu Rev Plant Biol 63:131–152

Korshunova Y, Eide D, Clark WG, Guerinot ML, Pakrasi H (1999) The IRT1 protein from *Arabidopsis thaliana* is a metal transporter with a broad substrate range. Plant Mol Biol 40:37–44

Lee T, Yang S, Kim E, Ko Y, Hwang S, Shin J et al (2015) AraNet v2: an improved database of co-functional gene networks for the study of *Arabidopsis thaliana* and 27 other nonmodel plant species. Nucleic Acids Res 43:D996–1002

Li J, Wu X-D, Hao S-T, Wang X-J, Ling H-Q (2008) Proteomic response to iron deficiency in tomato root. Proteomics 8:2299–2311

Li Y, Wang N, Zhao F et al (2014) Changes in the transcriptomic profiles of maize roots in response to iron-deficiency stress. Plant Mol Biol 85:349–363

Licciardello C, Torrisi B, Allegra M et al (2013) A transcriptomic analysis of sensitive and tolerant citrus rootstocks under natural iron deficiency conditions. J Am Soc Hortic Sci 138:487–498

Lin SI, Chiang SF, Lin WY et al (2008) Regulatory network of microRNA399 and PHO2 by systemic signaling. Plant Physiol 147:732–746

Liu J, Magalhaes JV, Shaff J, Kochian LV (2009) Aluminum-activated citrate and malate transporters from the MATE and ALMT families function independently to confer Arabidopsis aluminum tolerance. Plant J 57:389–399

Long TA, Tsukagoshi H, Busch W, Lahner B, Salt DE, Benfey PN (2010) The bHLH transcription factor POPEYE regulates response to iron deficiency in *Arabidopsis* roots. Plant Cell 22:2219–2236

López-Rayo S, Di Foggia M, Rodrigues Moreira E et al (2015) Physiological responses in roots of the grapevine rootstock 140 Ruggeri subjected to Fe deficiency and Fe-heme nutrition. Plant Physiol Biochem 96:171–179

Lowry OH, Rosebrough NJ, Farr AL, Randall RJ (1951) Protein measurement with the folin phenol reagent. J Biol Chem 193:265–275

Lucena C, Porras R, Romera FJ, Alcántara E, García MJ, Pérez-Vicente R (2018) Similarities and differences in the acquisition of Fe and P by dicot plants. Agronomy 8:148

Lv Q, Zhong Y, Wang Y et al (2014) SPX4 negatively regulates phosphate signaling and homeostasis through its interaction with PHR2 in rice. Plant Cell 26:1586–1597

Marschner H, Römheld V, Kissel M (1986) Different strategies in higher plants in mobilization and uptake of iron. J Plant Nutr 9:695–713

Martin M (2011) Cutadapt removes adapter sequences from high-throughput sequencing reads. EMBnet. J 17:10–12

Mendoza-Cózatl DG, Xie Q, Akmakjian GZ et al (2014) OPT3 is a component of the iron-signaling network between leaves and roots and misregulation of OPT3 leads to an over-accumulation of cadmium in seeds. Mol Plant 7:1455–1469

Mimmo T, Del Buono D, Terzano R et al (2014) Rhizospheric organic compounds in the soil-microorganism-plant system: their role in iron availability. Eur J Soil Sci 65:629–642

Nannipieri P, Ascher J, Ceccherini MT et al (2008) In: Nautiyal CS, Dion P (eds) Molecular mechanisms of plant and microbe coexistence. Springer, Berlin, pp 339–365

Neumann G, Römheld V (2011) Rhizosphere chemistry in relation to plant nutrition. In Marschner's mineral nutrition of higher plants. Academic Press, Massachusetts, pp 347–368

Nussaume L, Kanno S, Javot H et al (2011) Phosphate import in plants: focus on the PHT1 transporters. Front Plant Sci 2:83

O'Rourke JA, Nelson RT, Grant D et al (2009) Integrating microarray analysis and the soybean genome to understand the soybeans iron deficiency response. BMC Genom 10:376

O'Rourke JA, Yang SS, Miller SS et al (2013) An RNA-Seq transcriptome analysis of orthophosphate-deficient white lupin reveals novel insights into phosphorus acclimation in plants. Plant Physiol 161:705–724

Pfaffl MW (2001) A new mathematical model for relative quantification in real-time RT-PCR. Nucleic Acids Res 29:e45

Pfaffl MW, Horgan GW, Dempfle L (2002) Relative expression software tool (REST©) for group-wise comparison and statistical analysis of relative expression results in real-time PCR. Nucleic Acids Res 30:e36–e36

Pii Y, Cesco S, Mimmo T (2015) Shoot ionome to predict the synergism and antagonism between nutrients as affected by substrate and physiological status. Plant Physiol Biochem 94:48–56

Plaxton WC, Tran HT (2011) Metabolic adaptations of phosphate-starved plants. Plant Physiol 156:1006–1015

Puga MI, Mateos I, Charukesi R et al (2014) SPX1 is a phosphate-dependent inhibitor of phosphate starvation response 1 in *Arabidopsis*. Proc Natl Acad Sci USA 111:14947–14952

Raghothama KG (1999) Phosphate acquisition. Annu Rev Plant Biol 50:665–693

Ramakers C, Ruijter JM, Deprez RHL, Moorman AFM (2003) Assumption-free analysis of quantitative real-time polymerase chain reaction (PCR) data. Neurosci Lett 339:62–66

Rellán-Álvarez R, Andaluz S, Rodríguez-Celma J et al (2010) Changes in the proteomic and metabolic profiles of *Beta vulgaris* root tips in response to iron deficiency and resupply. BMC Plant Biol 10:120

Rodríguez-Celma J, Lattanzio G, Grusak MA, Abadía A, Abadía J, López-Millán A-F (2011) Root responses of *Medicago truncatula* plants grown in two different iron deficiency conditions: changes in root protein profile and riboflavin Biosynthesis. J Proteom Res 10:2590–2601

Rose TJ, Kretzschmar T, Liu L, Lancaster G, Wissuwa M (2016) Phosphorus deficiency alters nutrient accumulation patterns and grain nutritional quality in rice. Agronomy 6:52

Rouached H, Arpat AB, Poirier Y (2010) Regulation of phosphate starvation responses in plants: signaling players and cross-talks. Mol Plant 3:288–299

Sandnes A, Eldhuset TD, Wollebæk G (2005) Organic acids in root exudates and soil solution of Norway spruce and silver birch. Soil Biol Biochem 37:259–269

Santos CS, Silva AI, Serrão I, Carvalho AL, Vasconcelos MW (2013) Transcriptomic analysis of iron deficiency related genes in the legumes. Food Res Int 54:1162–1171

Schachtman DP (1998) Phosphorus uptake by plants: from soil to cell. Plant Physiol 116:447–453

Schmid NB, Giehl RFH, Döll S et al (2014) Feruloyl-CoA 6′-Hydroxylase1-dependent coumarins mediate iron acquisition from alkaline substrates in *Arabidopsis*. Plant Physiol 164:160–172

Secco D, Wang C, Arpat BA et al (2012) The emerging importance of the SPX domain-containing proteins in phosphate homeostasis. New Phytol 193:842–851

Secco D, Shou H, Whelan J, Berkowitz O (2014) RNA-seq analysis identifies an intricate regulatory network controlling cluster root development in white lupin. BMC Genom 15:230

Sharma T, Dreyer I, Kochian L, Piñeros MA (2016) The ALMT family of organic acid transporters in plants and their involvement in detoxification and nutrient security. Front Plant Sci 7:1488

Sivitz AB, Hermand V, Curie C, Vert G (2012) Arabidopsis bHLH100 and bHLH101 control iron homeostasis via a FIT-independent pathway. PLoS ONE 7:e44843

Tang H, Li X, Zu C, Zhang F, Shen J (2013) Spatial distribution and expression of intracellular and extracellular acid phosphatases of cluster roots at different developmental stages in white lupin. J Plant Physiol 170:1243–1250

Thimm O, Essigmann B, Kloska S, Altmann T, Buckhout TJ (2001) Response of *Arabidopsis* to iron deficiency stress as revealed by microarray analysis. Plant Physiol 127:1030–1043

Tian T, Liu Y, Yan H et al (2017) AgriGO v2.0: a GO analysis toolkit for the agricultural community, 2017 update. Nucleic Acids Res 45:W122–W129

Tomasi N, Mimmo T, Terzano R et al (2014) Nutrient accumulation in leaves of Fe-deficient cucumber plants treated with natural Fe complexes. Biol Fertil Soils 50:973–982

Trapnell C, Williams BA, Pertea G et al (2010) Transcript assembly and quantification by RNA-Seq reveals unannotated transcripts and isoform switching during cell differentiation. Nat Biotechnol 28:511–515

Trapnell C, Roberts A, Goff L et al (2012) Differential gene and transcript expression analysis of RNA-seq experiments with TopHat and Cufflinks. Nat Protoc 7:562–578

Valentinuzzi F, Cesco S, Tomasi N, Mimmo T (2015a) Influence of different trap solutions on the determination of root exudates in *Lupinus albus* L. Biol Fertil Soils 51:1–9

Valentinuzzi F, Mason M, Scampicchio M, Andreotti C, Cesco S, Mimmo T (2015b) Enhancement of the bioactive compound content in strawberry fruits grown under iron and phosphorus deficiency. J Sci Food Agric 95:2088–2094

Valentinuzzi F, Pii Y, Vigani G, Lehmann M, Cesco S, Mimmo T (2015c) Phosphorus and iron deficiencies induce a metabolic reprogramming and affect the exudation traits of the woody plant *Fragaria*×*ananassa*. J Exp Bot 66:6483–6495

Velasco R, Zharkikh A, Affourtit J et al (2010) The genome of the domesticated apple (*Malus*×*domestica* Borkh.). Nat Genet 42:833–839

Venuti S, Zanin L, Marroni F et al (2019) Physiological and transcriptomic data highlight common features between iron and phosphorus acquisition mechanisms in white lupin roots. Plant Sci 285:110

Wang N, Cui Y, Liu Y et al (2013) Requirement and functional redundancy of Ib subgroup bHLH proteins for iron deficiency responses and uptake in *Arabidopsis thaliana*. Mol Plant 6:503–513

Wang S, Lu B, Wu T et al (2014a) Transcriptomic analysis demonstrates the early responses of local ethylene and redox signaling to low iron stress in *Malus xiaojinensis*. Tree Genet Genomes 10:573–584

Wang Z, Straub D, Yang H et al (2014b) The regulatory network of cluster-root function and development in phosphate-deficient white lupin (*Lupinus albus*) identified by transcriptome sequencing. Physiol Plant 151:323–338

Wang Z, Ruan W, Shi J et al (2014c) Rice SPX1 and SPX2 inhibit phosphate starvation responses through interacting with PHR2 in a phosphate-dependent manner. Proc Natl Acad Sci USA 111:14953–14958

Waters BM, McInturf SA, Amundsen K (2014) Transcriptomic and physiological characterization of the *fefe* mutant of melon (*Cucumis melo*) reveals new aspects of iron-copper crosstalk. New Phytol 203:1128–1145

Wu P, Ma L, Hou X et al (2003) Phosphate starvation triggers distinct alterations of genome expression in *Arabidopsis* roots and leaves. Plant Physiol 132:1260–1271

Xiong H, Kakei Y, Kobayashi T et al (2013) Molecular evidence for phytosiderophore-induced improvement of iron nutrition of peanut intercropped with maize in calcareous soil. Plant Cell Environ 36:1888–1902

Yang XJ, Finnegan PM (2010) Regulation of phosphate starvation responses in higher plants. Ann Bot 105:513–526

Yuan Y, Wu H, Wang N et al (2008) FIT interacts with AtbHLH38 and AtbHLH39 in regulating iron uptake gene expression for iron homeostasis in *Arabidopsis*. Cell Res 18:385–397

Zamboni A, Zanin L, Tomasi N et al (2012) Genome-wide microarray analysis of tomato roots showed defined responses to iron deficiency. BMC Genom 13:101

Zancan S, Cesco S, Ghisi R (2006) Effect of UV-B radiation on iron content and distribution in maize plants. Environ Exp Bot 55:266–272

Zanin L, Tomasi N, Rizzardo C et al (2015) Iron allocation in leaves of Fe-deficient cucumber plants fed with natural Fe complexes. Physiol Plant 154:82–94

Zanin L, Venuti S, Tomasi N (2016) Short-term treatment with the urease inhibitor N-(n-butyl) thiophosphoric triamide (NBPT) alters urea assimilation and modulates transcriptional profiles of genes involved in primary and secondary metabolism in maize seedlings. Front Plant Sci 22:845

Zanin L, Venuti S, Zamboni A, Varanini Z, Tomasi N, Pinton R (2017) Transcriptional and physiological analyses of Fe deficiency response in maize reveal the presence of *Strategy I* components and Fe/P interactions. BMC Genom 18:154

Zanin L, Venuti S, Marroni F, Franco A, Morgante M, Pinton R, Tomasi N (2019) Physiological and RNA sequencing data of white lupin plants grown under Fe and P deficiency. Data in Brief 25:104069

Zeng H, Wang G, Zhang Y et al (2015) Genome-wide identification of phosphate-deficiency-responsive genes in soybean roots by high-throughput sequencing. Plant Soil 398:207–227

Zhai Z, Gayomba SR, Jung HI et al (2014) OPT3 is a phloem-specific iron transporter that is essential for systemic iron signaling and redistribution of iron and cadmium in *Arabidopsis*. Plant Cell 26:2249–2264

Zhang J-H, Mao Z-Q, Wang L-Q, Shu H-R (2007) Bioassay and identification of root exudates of three fruit tree species. J Integr Plant Biol 49:257–261

Zhang F, Shen J, Zhang J, Zuo Y, Li L, Chen X (2010) Rhizosphere processes and management for improving nutrient use efficiency and crop productivity: implications for China. Elsevier, Amsterdam

Zheng L, Huang F, Narsai R et al (2009) Physiological and transcriptome analysis of iron and phosphorus interaction in rice seedlings. Plant Physiol 151:262–274